C. R. Physique 14 (2013) 53–77

Contents lists available at SciVerse ScienceDirect

Comptes Rendus Physique

www.sciencedirect.com

Physics in High Magnetic Fields / Physique en champ magnétique intense

Heavy fermions in a high magnetic field

Fermions lourds en champ magnétique intense

Dai Aoki [a,*], William Knafo [b], Ilya Sheikin [c]

[a] *Institut nanosciences et cryogénie, SPSMS, CEA-Grenoble, 17, rue des Martyrs, 38054 Grenoble cedex 9, France*
[b] *Laboratoire national des champs magnétiques intenses, UPR 3228, CNRS–UJF–UPS–INSA, 143, avenue de Rangueil, 31400 Toulouse, France*
[c] *Laboratoire national des champs magnétiques intenses, UPR 3228, CNRS–UJF–UPS–INSA, 25, rue des Martyrs, B.P. 166, 38042 Grenoble cedex 9, France*

ARTICLE INFO

Article history:
Available online 30 January 2013

Keywords:
Heavy fermions
High magnetic field
Metamagnetism
Fermi surface
Ferromagnetic superconductors

Mots-clés :
Fermions lourds
Champ magnétique intense
Métamagnétisme
Surface de Fermi
Supraconducteurs ferromagnétiques

ABSTRACT

We give an overview on experimental studies performed in the last 25 years on heavy-fermion systems in a high magnetic field. The properties of field-induced magnetic transitions in heavy-fermion materials close to a quantum antiferromagnetic-to-paramagnetic instability are presented. Effects of a high magnetic field to the Fermi surface, in particular the splitting of spin-up and spin-down bands, are also considered. Finally, we review on recent advances on the study of non-centrosymmetric compounds and ferromagnetic superconductors in a high magnetic field.

RÉSUMÉ

Cette revue donne un aperçu des études expérimentales faites depuis 25 ans sur les systèmes à fermions lourds en champ magnétique intense. Les propriétés des transitions de phase magnétiques de composés proches d'une instabilité antiferromagnétique sont présentées. Les effets d'un champ magnétique intense sur la surface de Fermi, en particulier la séparation des bandes de spin « up » et « down », sont aussi considérées. Finalement, nous faisons le point sur les avancées récentes dans l'étude en champ magnétique intense de composés non centrosymétriques et de supraconducteurs ferromagnétiques.

1. Introduction

Heavy-fermion systems [1,2] are intermetallic materials composed of rare earths (Ce, Yb) or actinides (U, Np, Pu) elements. In these systems, partially filled $4f$- or $5f$-electron orbitals are strongly-coupled to conduction-electrons bands. Electronic interactions give rise to the formation of heavy quasiparticles, i.e., narrow electronic bands with a strong enhancement of the effective mass m^*, which typically reaches 100 to 1000 times the value of the free-electron mass m_0. The magnetic properties of heavy fermions are governed by a subtle competition between Kondo and Ruderman–Kittel–Kasuya–Yosida (RKKY) interactions, both of which depending on the product of the exchange interaction J between an f-electron and a conduction electron by the density $n(E_F)$ of states at the Fermi level. The Kondo interaction can be seen as a screening of f-electron magnetic moments by the conduction electrons, which tends to destabilize the magnetic ordering of the f-electron moments. Its characteristic energy scale, the Kondo temperature, can be approximated by:

* Corresponding author.
E-mail addresses: dai.aoki@cea.fr (D. Aoki), william.knafo@lncmi.cnrs.fr (W. Knafo), ilya.sheikin@lncmi.cnrs.fr (I. Sheikin).

1631-0705/$ – see front matter
http://dx.doi.org/10.1016/j.crhy.2012.11.004

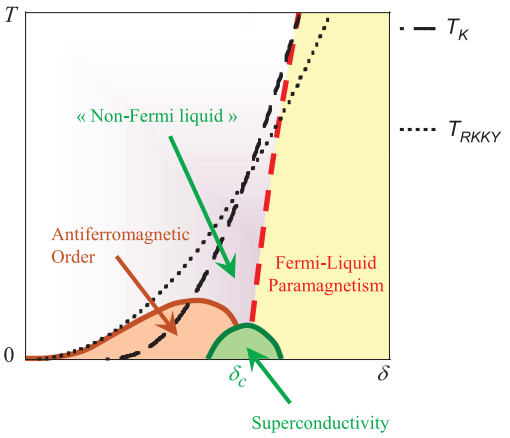

Fig. 1. Doniach's phase diagram. The short dashed line is the RKKY temperature, T_{RKKY}, at which magnetic order would occur in the absence of the Kondo screening. The long dashed line is the Kondo temperature, T_K, below which the f-electron moments are screened by the conduction electrons. When $T_{RKKY} = T_K$, the magnetic ordering temperature is driven to zero giving rise to a quantum phase transition between an antiferromagnetic and a paramagnetic Fermi liquid ground states. In many heavy-fermion systems, a superconducting pocket develops in the vicinity of the quantum phase transition.

$$T_K \propto \exp\bigl(-1/Jn(E_F)\bigr) \tag{1}$$

The RKKY interaction is a magnetic exchange interaction between the f-electron moments mediated by the conduction electrons, which promotes long-range magnetic ordering. Its energy scale, the RKKY temperature, can be approximated by:

$$T_{RKKY} \propto J^2 n(E_F) \tag{2}$$

The parameter $\delta = Jn(E_F)$ can be varied by applying either hydrostatic or chemical pressure. In many systems, it is possible to drive by pressure or doping the magnetic ordering temperature to zero, giving rise to a quantum phase transition (in the limit of zero temperature) between an antiferromagnetic and a paramagnetic ground states. Doniach's phase diagram [3,4] drawn in Fig. 1 schematically illustrates how the competition of Kondo and RKKY interactions can lead to an antiferromagnetic-to-paramagnetic quantum instability. In the vicinity of the quantum phase transition, the amplitude of quantum magnetic fluctuations grows rapidly, leading to two distinct phenomena: non-Fermi liquid behavior [5] and unconventional superconductivity [6]. A non-Fermi liquid is a strong deviation from a Fermi liquid behavior at low temperature, observed in resistivity [$\rho(T) = \rho_0 + AT^n$, $1 < n < 1.5$ instead of $\rho(T) = \rho_0 + AT^2$], magnetic susceptibility [sometimes $\chi(T) \propto \chi_0(1 - c(T/T_0)^{1/2})$ instead of $\chi(T) = \chi_0(1 + aT^2)$] and specific heat (sometimes $C/T \propto -\ln T$ instead of $C/T = \gamma + \beta T^2$) measurements. Interplay between magnetism and superconductivity is at the heart of the heavy-fermion problem, since unconventional superconductivity often develops in the vicinity of a quantum phase transition [6], being only observed in very clean heavy-fermion samples. Electron pairing is probably due to quantum critical magnetic fluctuations (instead of phonons as in conventional superconductors), whose intensity is maximal at the quantum phase transition. The question of the nature of quantum critical magnetic fluctuations is still a matter of strong debate. A scenario based on critical fluctuations of the magnetic order parameter has initially been proposed [7–9], but it failed to describe the non-Fermi liquid regime. An unconventional scenario based on local, i.e., wave vector **q**-independent, critical magnetic fluctuations has also been proposed by some authors [10]. More recently, an enhancement of the antiferromagnetic fluctuations, but not of the local magnetic fluctuations, was observed at the quantum phase transition in the heavy-fermion system $Ce_{1-x}La_xRu_2Si_2$ [11] permitting to rehabilitate, at least for this system, the conventional scenario based on quantum critical fluctuations of the order parameter. Another issue is to determine whether the f-electrons are itinerant or localized on both sides of the quantum phase transition. This can be achieved by comparing the experimentally-obtained angular dependence of de Haas–van Alphen frequencies with the results of theoretical band structure calculations performed for both itinerant and localized f-electrons. De Haas–van Alphen measurements also provide the effective masses for each band, whose behavior on crossing a quantum phase transition can be investigated.

While many heavy fermions have been initially studied under pressure and/or doping, these last years have shown the emergence of numerous works under a magnetic field **H**. The three main phenomena associated with pressure- or doping-induced quantum criticality have been already observed in a magnetic field, i.e. (i) field-induced non-Fermi liquid (e.g. in $YbRh_2Si_2$ [12]), (ii) field-induced quantum critical fluctuations (of ferromagnetic nature in $CeRu_2Si_2$ [13–15]), and (iii) field-induced superconductivity (in URhGe [16,17]). Contrary to pressure and doping, a magnetic field can be easily varied continuously. Under a magnetic field, heavy-fermion systems undergo a transition to a polarized paramagnetic regime. The three-dimensional phase diagram (δ, H, T) shown in Fig. 2 illustrates schematically how the polarized regime is reached from the zero-field antiferromagnetic or paramagnetic ground states. The present review aims to give an overview of recent state-of-art studies of heavy fermions in a magnetic field, with a particular focus on experiments performed in very high

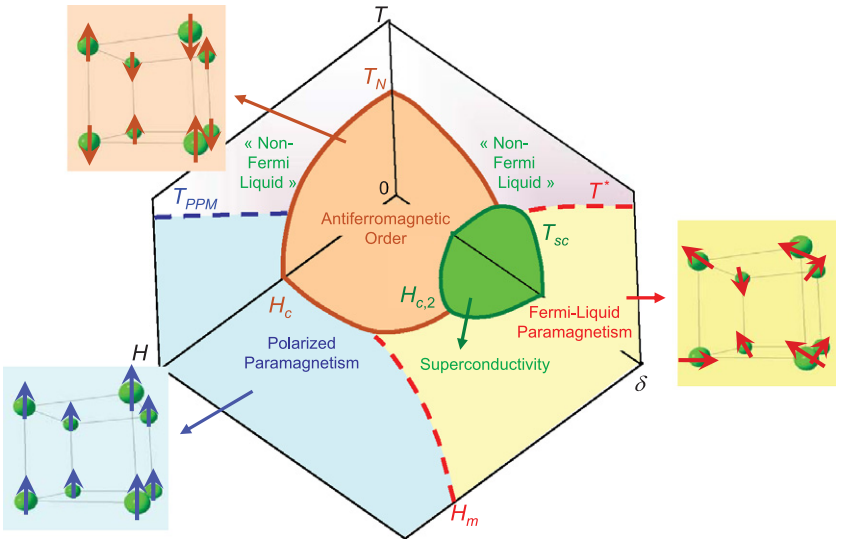

Fig. 2. Schematic three-dimensional (T, δ, H) phase diagram of heavy-fermion systems close to an antiferromagnetic-to-paramagnetic quantum instability, where δ can be the pressure or a doping.

fields above 20 T. Section 2 focuses on field-induced quantum criticality in heavy-fermion systems close to an antiferromagnetic instability. The magnetic and Fermi surface properties at a quantum phase transition under magnetic field will be considered for heavy-fermion antiferromagnets and paramagnets, including the exotic 'hidden-order' material URu_2Si_2. Magnetic field is expected to modify the magnetic correlations and, therefore, the electronic structure of heavy-fermion compounds, i.e., the Fermi surface topology and effective masses. The study of heavy-fermion Fermi surfaces in a high field is considered in detail in Section 3, where the splitting by a magnetic field of the Fermi surface into majority-spin and minority-spin surfaces, with different spin-up and spin-down effective masses, as predicted by most theoretical models, is considered. Following the discovery of superconductivity in the non-centrosymmetric heavy-fermion compound $CePt_3Si$ [18], materials without inversion symmetry in their crystal structure have attracted a lot of experimental and theoretical interest. The interest is mainly due to a fascinating theoretical prediction [19,20] that superconductive pairing in such systems requires an admixture of a spin-singlet with a spin-triplet state. Very unusual superconducting properties of these materials, such as enormously high upper critical field, will be discussed in Section 4. Finally, Section 5 synthesizes the high-field properties of the recently discovered class of ferromagnetic superconductors. This family is composed of UGe_2 [21], URhGe [22], UIr [23], and UCoGe [24]. While UGe_2 and UIr become superconducting under pressure, URhGe and UCoGe are superconducting at ambient pressure, well below their Curie temperature. Field-induced superconductivity develops in URhGe around a field of 12 T applied along **b**, which is well above the critical superconducting field of 2.5 T [16], and results from the presence of a field-induced magnetic transition.

2. Field-induced magnetic transitions

Field-induced magnetic transitions have been observed in many heavy-fermion materials with either a paramagnetic or a magnetically-ordered ground state. Among the former are, for example, the prototypical $CeRu_2Si_2$ [25,26] and $CeCu_6$ [27,28] heavy-fermion paramagnets. The latter include $CeRh_2Si_2$ [29], $CePd_2Si_2$ [30], and $YbRh_2Si_2$ [31]. In many systems, a strong magnetic anisotropy leads at low temperature to field-induced first-order transitions. Such transitions, called metamagnetic transitions, are characterized by a sudden step-like increase of the magnetization at the onset of polarized paramagnetism [32]. As pointed out for itinerant magnets [33,34] and heavy-fermion magnets [35–39], which are a sub-class of itinerant magnets, the transition field is often related to the temperature $T_\chi^{\max}$ at the maximum of the magnetic susceptibility by a correspondence 1 T $\leftrightarrow$ 1 K. From the Maxwell relation $(\partial M/\partial T)_H = (\partial S/\partial H)_T$, the magnetic entropy S and thus the magnetic fluctuations increase with the magnetic field H when the temperature is smaller than $T_\chi^{\max}$, indicating the proximity of a field-induced transition [40]. A maximum in the magnetic susceptibility at low magnetic field, as shown in Fig. 3 for several heavy-fermion paramagnets and antiferromagnets [41], is thus generally the first indication for a high-field transition. A metamagnetic transition can also be driven to zero temperature [42] by tuning an additional parameter, leading to a quantum critical end point (cf. the bilayer ruthenate $Sr_3Ru_2O_7$ [43,44], where the field-tuned quantum critical point also leads to new – and not yet identified – low-temperature phases). In this section we present an overview of field-induced magnetic transitions in heavy-fermion materials close to a paramagnetic-to-antiferromagnetic instability (the case of ferromagnetic heavy fermions will be considered separately in Section 5). Section 2.1 presents the high-field properties of paramagnetic systems and Section 2.2 is devoted to heavy-fermion antiferromagnets. Section 2.3 shows that Fermi surface modifications can be induced at a heavy-fermion field-induced transition. Finally, Section 2.4 focuses on the exotic case of

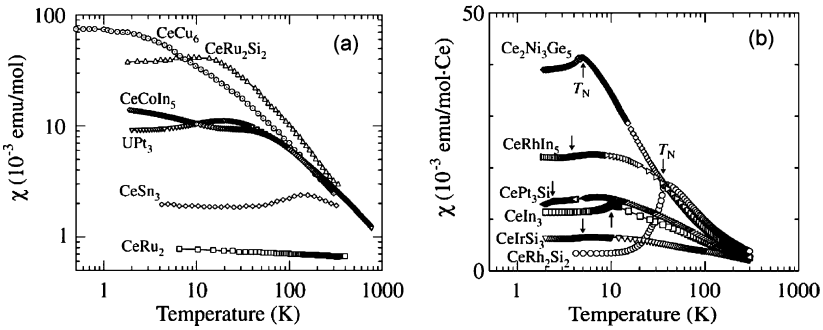

Fig. 3. Magnetic susceptibility of various heavy-fermion (a) paramagnets and (b) antiferromagnets [41] (Copyright 2007 The Physical Society of Japan).

Table 1
Temperature of the maximum (or kink) in the magnetic susceptibility, magnetic field of the transition, field direction, and inelastic neutron scattering linewidth in various heavy-fermion paramagnets.

Material	$T_\chi^{\max}$ (K)	$\mu_0 H_m$ (T)	**H** ∥	Linewidth Γ (K)	References
$CeRu_2Si_2$	10	7.8	**c**	10 ($\mathbf{k}_1, T \to 0$)	[11,45–47]
$CeRu_2Si_2$ ($p = 1 \to 2$ kbar)	11.7 → 14	10.3 → 13	**c**	–	[48]
$Ce_{1-x}Y_xRu_2Si_2$ ($x = 1.5 \to 10\%$)	12.5 → 25	9.5 → 19.3	**c**	–	[49,50]
$Ce_{1-x}La_xRu_2Si_2$ ($x = 3 \to 7.5\%$)	7.4 → 5	6.2 → 4	**c**	– → 2.5 ($\mathbf{k}_1, T \to 0$)	[45,51–53]
$CeRu_2(Si_{1-x}Ge_x)_2$ ($x = 3.5 \to 7\%$)	6 → 3.8	6 → 4.2	**c**	–	[54]
$CeFe_2Ge_2$	(kink at ≃ 20 K)	30	**c**	–	[55,56]
$CeNi_2Ge_2$	28	42 (powder)	**c**	40 ($\mathbf{q}_0, T \to 0$)	[36,57]
$CeIrIn_5$	(kink at ≃ 30 K)	30–40	**c**	30 ($\langle\mathbf{Q}\rangle$, $T = 8$ K)	[58–60]
$CeCu_6$	(kink at ≃ 1–1.5 K)	1.7	**c**	2.5 ($(1.15, 0, 0), T \to 0$)	[27,28,61]
CeTiGe	25	12.5	(polycrystal)	–	[62]
CeFePO	5	4	**c**	–	[63]
$YbIr_2Zn_{20}$	7.4	9.7 (12)	[100] ([110])	–	[39]
$YbRh_2Zn_{20}$	5.3	6.4	[100]	–	[64]
$YbCo_2Zn_{20}$	0.32	0.6 (0.57)	[100] ([110])	–	[64,65]
$YbCu_{5-x}Ag_x$ ($x = 0 \to 1$)	17 → 40	10 → 40	(cubic)	–	[66,67]
USn_3	(kink at ≃ 15–20 K)	30	**a**	60 ($\langle\mathbf{Q}\rangle$)	[37,68]
URu_2Si_2	55	35–39	**c**	50 ($\mathbf{Q}_1, T \geqslant T_0$)	[35,69,70]

URu_2Si_2 where the hidden-order state, whose unknown nature is still a matter of strong debate, can be destabilized by a high magnetic field.

2.1. Heavy-fermion paramagnets

Table 1 summarizes the characteristics of several heavy-fermion paramagnets undergoing a field-induced transition to a polarized paramagnetic regime. In this table, the metamagnetic (called sometimes pseudo-metamagnetic when the transition is not clearly first-order) field H_m, the temperature $T_\chi^{\max}$ at the maximum of the susceptibility, and the corresponding field direction are given for each system. Fig. 4 presents in a log–log scale a H_m versus $T_\chi^{\max}$ plot of these data. It extends to a higher number (≃ 30) of heavy-fermion materials the similar plots already presented in Refs. [35–39,64], and is restricted here to paramagnets. A H_c versus T_N plot will be shown for heavy-fermion antiferromagnets in Section 2.2. A striking feature of Fig. 4 is that H_m and $T_\chi^{\max}$ are almost connected by a simple correspondence 1 T ↔ 1 K. Most of the compounds considered are such that $0.8 \cdot T_\chi^{\max} < \mu_0 H_m < 1.6 \cdot T_\chi^{\max}$, despite H_m and $T_\chi^{\max}$ vary by more than two decades, from 0.57 T and 0.32 K, respectively, in $YbCo_2Zn_{20}$ (**H** ∥ [110]) to 35–39 T and 55 K, respectively, in URu_2Si_2 (**H** ∥ **c**). The fact that H_m and $T_\chi^{\max}$ are almost linearly connected indicates that they are mainly controlled by a single energy scale. In the literature (see for example Refs. [35,37–39,64]), it has often been proposed that $T_\chi^{\max}$ in heavy-fermion paramagnets is related to the onset of the Kondo hybridization between f- and conduction electrons, i.e., to a crossover from a high-temperature regime where the f-electrons are localized to a low-temperature regime where they are itinerant. This hypothesis is compatible with the assumption proposed in Ref. [63] that the metamagnetic field H_m in CeFePO is associated with a breakdown of the Kondo effect. These hypotheses assume that $T_\chi^{\max}$ and H_m are respectively related to the temperature- and magnetic field-induced destruction of the Kondo hybridization, as expected from a single-impurity Kondo model [72,73]. They also imply that a drastic reduction of **q**-independent Kondo magnetic fluctuations [11] should occur for $T > T_\chi^{\max}$ and $H > H_m$, respectively, which has never been shown experimentally yet. Other theories have been proposed to describe metamagnetism in heavy-fermion paramagnets, from single-site models [74–78] to models where intersite correlations are also considered [79–81]. We show below that neutron experiments on the heavy-fermion paramagnet $CeRu_2Si_2$ indicate that $T_\chi^{\max}$ and H_m in this system are related to intersite antiferromagnetic correlations, but not to the Kondo effect.

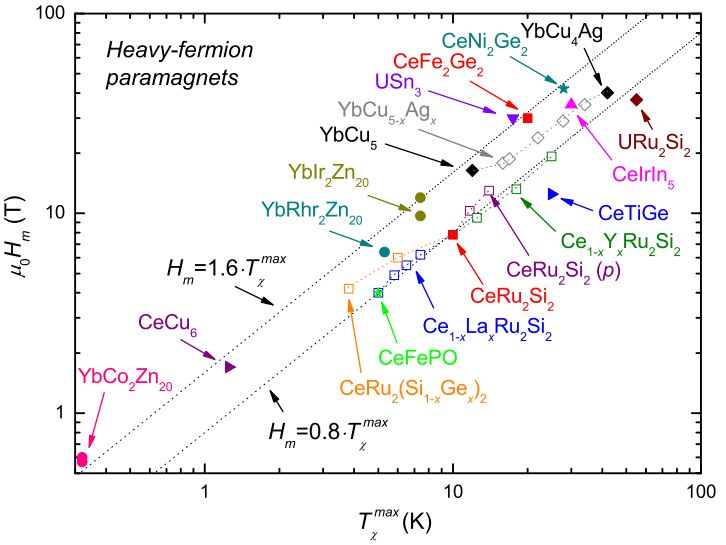

Fig. 4. Metamagnetic field as a function of the temperature at the maximum (or kink) of the magnetic susceptibility for various heavy-fermion paramagnets [27,28,35–37,45,46,48–50,55,56,58,59,62,69,71].

$CeRu_2Si_2$ has been one of the mostly-studied heavy-fermion systems since twenty years. The proximity of this paramagnet to antiferromagnetic instabilities is demonstrated by the increase on cooling of the specific heat divided by temperature C_p/T [45] and of the electronic Grüneisen parameter [82]. RKKY interactions lead to maxima of the dynamical magnetic susceptibility at the incommensurate wave vectors $\mathbf{k}_1 = (0.31, 0, 0)$, $\mathbf{k}_2 = (0.31, 0.31, 0)$, and $\mathbf{k}_3 = (0, 0, 0.35)$, as probed by inelastic neutron scattering [83]. At wave vectors sufficiently far from $\mathbf{k}_1$, $\mathbf{k}_2$, and $\mathbf{k}_3$ magnetic fluctuations persist and can be considered as the signature of a local (or single-site) Kondo effect. Chemical doping (with La, Ge, or Rh) and/or magnetic field tunings can favor one particular interaction and establish antiferromagnetic long-range ordering with either $\mathbf{k}_1$, $\mathbf{k}_2$, or $\mathbf{k}_3$ wave vectors [84–87]. Upon doping by La, it has been shown that the quantum phase transition to an antiferromagnetic state is governed by fluctuations of the antiferromagnetic order parameter (moment with the wave vector $\mathbf{k}_1$) [11]. Under a magnetic field applied along the easy axis $\mathbf{c}$, a magnetic transition to a polarized paramagnetic regime occurs at $\mu_0 H_m = 7.8$ T [46] [Figs. 5(a), (b)]. As well as the temperature T_α^{max} at the maximum of thermal expansion [46], the temperature T_χ^{max} at the maximum of susceptibility [88] decreases in a magnetic field $\mathbf{H} \parallel \mathbf{c}$ and vanishes above H_m. T_χ^{max} and T_α^{max} are related to the same phenomenon and they delimitate a low-temperature regime which vanishes above H_m [89]. The correspondence 1 K $\leftrightarrow$ 1 T between $T_\chi^{max} = 10$ K and H_m in $CeRu_2Si_2$ suggests that both are controlled by a single magnetic energy scale. Antiferromagnetic fluctuations at $\mathbf{k}_1$ vanish at H_m, while ferromagnetic fluctuations develop in a narrow window around H_m [13–15] [Fig. 5(c)]. At zero field, antiferromagnetic fluctuations with $\mathbf{k}_1$ saturate below $\simeq 10$ K and their temperature scale is given by the linewidth $\Gamma(\mathbf{k}_1) = 10\ \text{K} = T_\chi^{max}$ [11,47]. T_χ^{max} and H_m correspond thus to the energy scale of the antiferromagnetic fluctuations with the wave vector $\mathbf{k}_1 = (0.31, 0, 0)$ and the regime below T_χ^{max} and H_m is controlled by these intersite magnetic fluctuations. When crossing T_χ^{max} or H_m, no drastic change of local ($\mathbf{q}$-independent) Kondo magnetic fluctuations has been observed [11,14,47], which indicates that no sudden modification of the single-site Kondo effect and thus no Kondo breakdown occur at T_χ^{max} or H_m.

$CeRu_2Si_2$ is a unique heavy-fermion compound which has been investigated on both sides of its metamagnetic transition by a full set of experimental techniques made of electronic transport, thermodynamic, elastic and inelastic neutron scattering, de Haas–van Alphen, and X-rays absorption spectroscopy experiments (see also Section 2.3). Contrary to $CeRu_2Si_2$, the magnetic fluctuations of other heavy-fermion systems across their metamagnetic transition have not yet been systematically investigated by neutron scattering. However, inelastic neutron scattering at zero field permitted to extract the antiferromagnetic linewidth for $Ce_{0.925}La_{0.075}Ru_2Si_2$ [11,53], $CeNi_2Ge_2$ [57], $CeCu_6$ [61], and URu_2Si_2 [70], whose value is rather close to the value of T_χ^{max}, as in $CeRu_2Si_2$ (see Table 1). In $CeIrIn_5$ [60] and USn_3 [68], the linewidth measured on an averaged wave vector $\langle \mathbf{Q} \rangle$ is also similar to T_χ^{max} (see Table 1), but it is not known whether this linewidth results from an intersite Q-dependent signal or a local Q-independent signal. To test if H_m and T_χ^{max} are controlled by the onset of antiferromagnetic correlations in these systems, inelastic neutron scattering might be performed systematically to check whether antiferromagnetic correlations disappear above H_m (as in $CeRu_2Si_2$) or if a different behavior could be observed. As emphasized in [69], the case of URu_2Si_2 above its hidden-order temperature $T_0 = 17.5$ K looks rather similar to the $CeRu_2Si_2$ case, since the extrapolation of neutron data (measured up to 17 T) is compatible with a loss of antiferromagnetic correlations above 35 T [90] (cf. also Section 2.4).

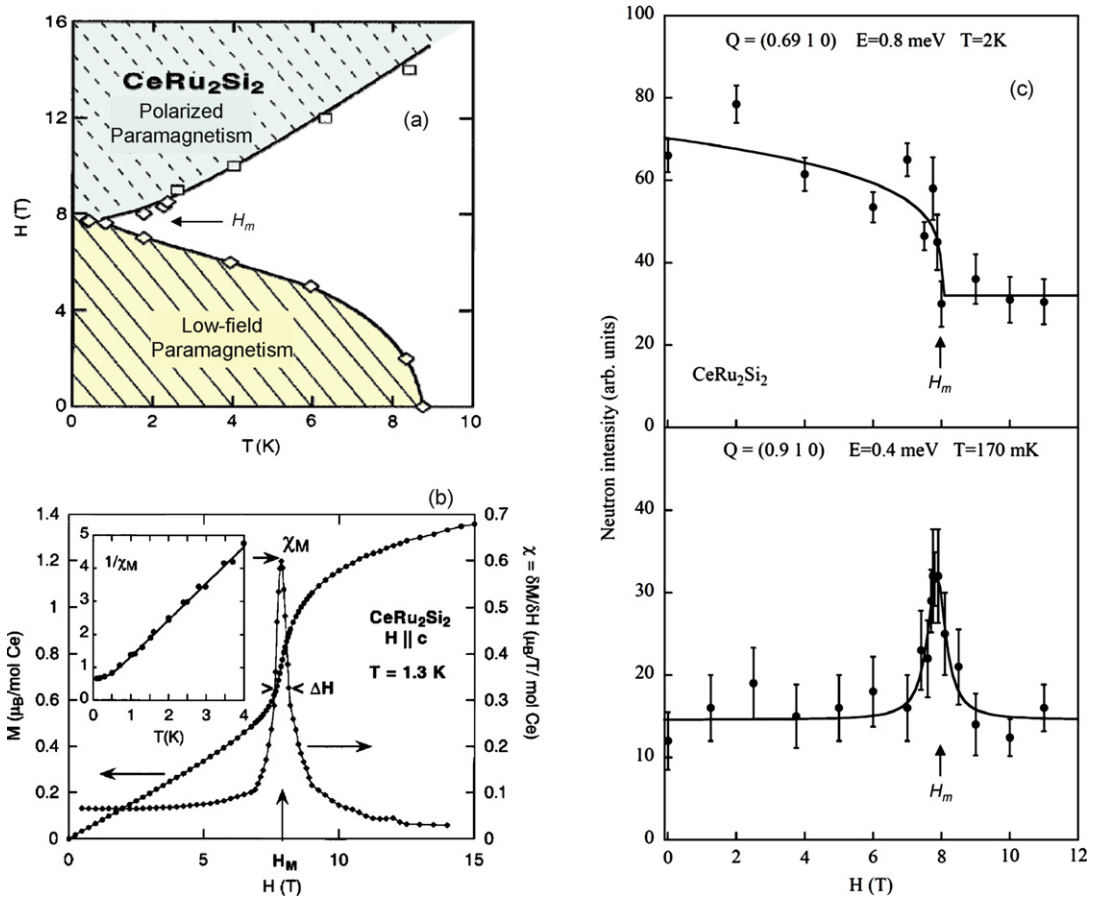

Fig. 5. (a) (T, δ, H) phase diagram probed by thermal expansion and heat capacity showing a low-field paramagnetic regime and a high-field polarized paramagnetic regime separated by $\mu_0 H_m = 8$ T [26], (b) magnetization versus field [26] (Copyright 2002 Elsevier), and (c) inelastic neutron scattering intensity at wave vectors characteristic of the antiferromagnetic (top) and ferromagnetic (bottom) fluctuations [15] (Copyright 2004 Elsevier), of $CeRu_2Si_2$ with $\mathbf{H} \parallel \mathbf{c}$.

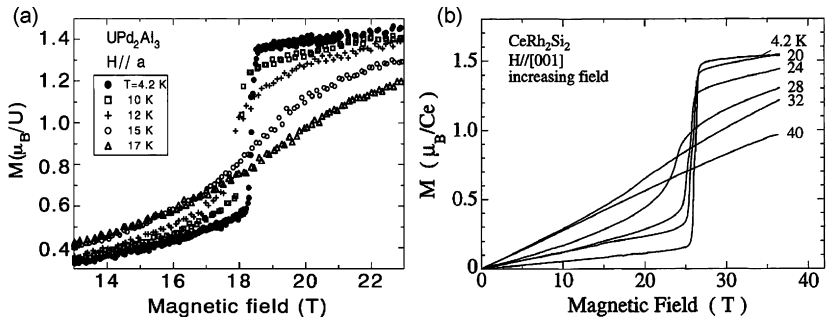

Fig. 6. High-field magnetization of (a) UPd_2Al_3 [91] (Copyright 2002 The Japan Society of Applied Physics) and (b) $CeRh_2Si_2$ [92] (Copyright 1997 The Physical Society of Japan).

2.2. Heavy-fermion antiferromagnets

Due to a strong anisotropy, the field-induced transition of heavy-fermion antiferromagnets is often first-order, being accompanied by a sudden step-like change in the magnetization. In UPd_2Al_3, antiferromagnetism sets up below $T_N = 14$ K and a first-order transition is induced at $\mu_0 H_c = 18.4$ T for $\mathbf{H} \parallel \mathbf{a}$ [91] [Fig. 6(a)]. As shown in Fig. 7(c), the antiferromagnetic-to-paramagnetic borderline of UPd_2Al_3 is of second order at high temperature and becomes first-order at low temperature. Such a change from second to first order is also reported in other heavy-fermion antiferromagnets, as $CeRh_2Si_2$ [29] [Fig. 7(b)]. In this system, the Néel temperature $T_N = 36$ K is one of the highest in the heavy-fermion family and a cascade of two field-induced first-order phase transitions develops below 20 K, with presumably an antiferromagnetic canted phase

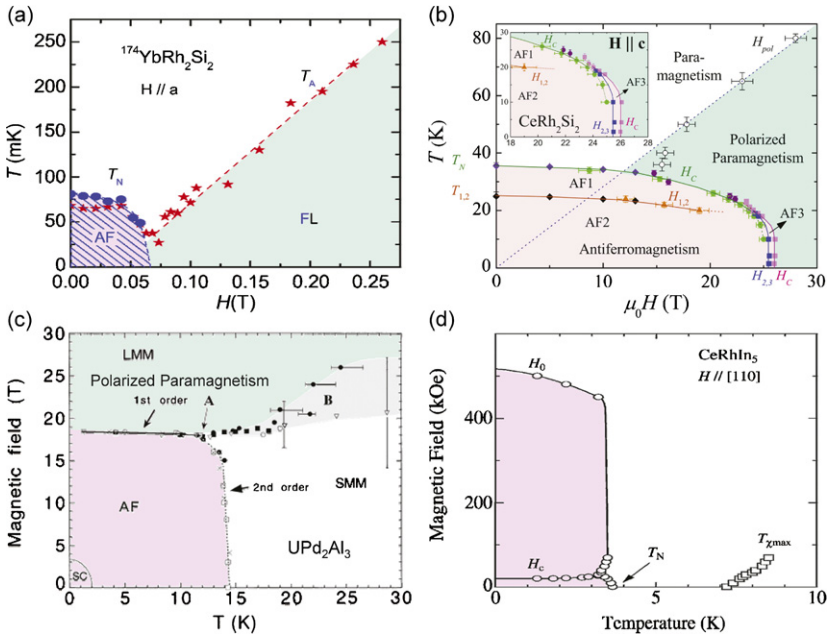

Fig. 7. Magnetic field–temperature phase diagrams of (a) $YbRh_2Si_2$ [93] (Copyright 2006 The Physical Society of Japan), (b) $CeRh_2Si_2$ [29], (c) UPd_2Al_3 [91] (Copyright 2002 The Japan Society of Applied Physics), with **H** ∥ **c**, and (d) $CeRhIn_5$ with **H** ⊥ **c** [59] (Copyright 2001 The Physical Society of Japan).

Table 2
Néel temperature, critical magnetic field, and field direction for the metamagnetic transition in various heavy-fermion antiferromagnets.

Material	T_N (K)	$\mu_0 H_c$ (T)	**H** ∥	References
$Ce_{1-x}La_xRu_2Si_2$ ($x = 16 \to 70\%$)	$5.4 \to 3.2$	$3.4 \to 1$	**c**	[51,52,86]
$CeRu_2(Si_{1-x}Ge_x)_2$ ($x = 10 \to 52\%$)	$6.6 \to 10.4$	$3 \to 0.4$	**c**	[54,86]
$Ce(Ru_{0.92}Rh_{0.08})_2Si_2$	4	3	**c**	[96]
$CeCu_2Ge_2$	4	8	[1̄10]	[97]
$CeRh_2Si_2$	36	26	**c**	[29]
$CeIn_3$	10	61	(cubic)	[98]
$CeIn_{2.75}Sn_{0.25}$	6.4	42	(cubic)	[99]
$CeRhIn_5$	3.8	2/52	[110]	[59]
$YbRh_2Si_2$	0.07	0.06	**c**	[93]
Yb_3Pt_4	2.4	1.85	⊥ **c**	[100]
$YbNiSi_3$	5.1	8.3 (9)	**b** (⊥ **b**)	[94,95]
U_2Zn_{17}	9.7	32	[11$\bar{2}$0]	[101]
UPd_2Al_3	14	18.4	**a**	[91]
UPb_3	32	21	**a**	[37]
UPt_2Si_2	32	45 (32)	**a** (**c**)	[102]

stabilized between 25.5 and 26 T [92] [Fig. 6(b)]. Some exceptions, as $YbNiSi_3$, behave in a magnetic field as 'textbook' localized and almost-isotropic antiferromagnets: $YbNiSi_3$ is characterized by a spin-flop transition at 1.7 T, when the field is applied along the easy magnetic axis **b**, and gets polarized above similar critical fields of 8.3 and 9.5 T, when the field is applied along and perpendicularly to **b**, respectively [94,95]. For comparison with the cases of $CeRh_2Si_2$ and UPd_2Al_3, where the magnetic energy scales are high [several tens of K or T, see Figs. 7(b), (c)], Fig. 7(a) shows the magnetic field–temperature phase diagram of $YbRh_2Si_2$, which has extremely small temperature and magnetic scales $T_N = 70$ mK and $\mu_0 H_c = 60$ mT, respectively [93]. It comes out that for $YbRh_2Si_2$, $CeRh_2Si_2$, and UPd_2Al_3, despite very different – by a factor 500 – energy scales, the critical field H_c and the Néel temperature T_N scale rather well within a correspondence 1 T ↔ 1 K. In these three systems, a characteristic temperature of the high-field regime ($H > H_c$) increases almost linearly with H, being presumably related to the Zeeman energy.

Table 2 lists the values of $T_N(H = 0)$ and $H_c(T \to 0)$ for different heavy-fermion antiferromagnets. T_N and H_c are believed to be controlled by the same exchange interactions, since the H_c line is the continuation of the T_N line in the (H, T) plane. It is thus natural to plot (in a log–log scale) H_c versus T_N in Fig. 8 instead of H_c versus T_χ^{max} as in Fig. 4 (cf. also [35–39]). Similarly to the H_m versus T_χ^{max} plot made for heavy-fermion paramagnets in Fig. 4, the H_c versus T_N plot shows that these two quantities are roughly related by a correspondence 1 T ↔ 1 K, which indicates that they are mainly controlled by one energy scale. However, the scattering of the data points in the H_c versus T_N plot (Fig. 8) is more important than that in the H_m versus T_χ^{max} plot (Fig. 4): most of the heavy-fermion antiferromagnets considered here are such that

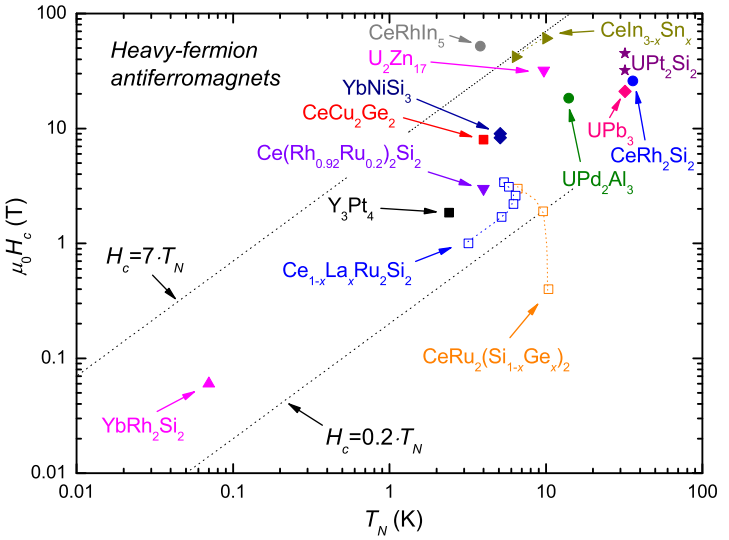

Fig. 8. Critical field as a function of the Néel temperature of various heavy-fermion antiferromagnets [29,86,91,93,95–101].

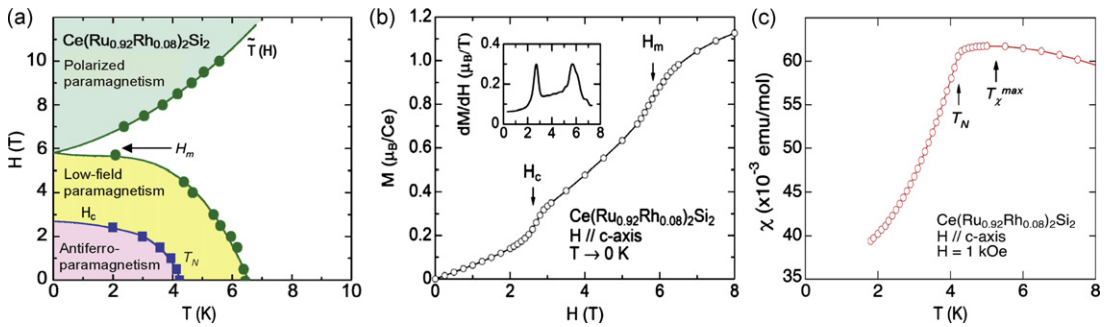

Fig. 9. (a) Magnetic field–temperature phase diagram showing a low-field antiferromagnetic regime below $\mu_0 H_c = 3$ T, a low-field paramagnetic regime between H_c and $\mu_0 H_m = 6$ T, and a high-field polarized paramagnetic regime above H_m, (b) magnetization versus field and (c) magnetic susceptibility versus temperature of $Ce(Rh_{0.92}Ru_{0.08})_2Si_2$ with $\mathbf{H} \parallel \mathbf{c}$ [96].

$0.2 \cdot T_N < \mu_0 H_c < 7 \cdot T_N$, when H_c and T_N vary by almost three orders of magnitude. This strong deviation from a unique scaling law illustrates the necessity to considerer several parameters to describe heavy-fermion antiferromagnetism, instead of a single parameter if H_c and T_N would have fallen in a simple and unique law for all systems. Additional parameters like multiple exchange paths, the dimensionality of these exchange couplings, the magnetic anisotropy, could explain the strong scattering of the data points in Fig. 8. For example, the case of $CeRhIn_5$ [59], which is antiferromagnetically ordered below $T_N = 3.8$ K, deviates strongly from the 'mean' behavior of other heavy-fermion antiferromagnets: as shown in Fig. 7(c), its phase diagram for $\mathbf{H} \parallel [110]$ is composed of two field-induced phase transitions at 2 and 52 T. A factor $\simeq 14$ T/K instead of a 'mean' slope $\simeq 1$ T/K relates the upper critical field to T_N. A low-dimensionality of the magnetic interactions proposed in [59] to describe the field-induced increase of T_χ^{max} in $CeRhIn_5$, could also explain the strong deviation found here.

In heavy-fermion antiferromagnets, T_χ^{max} is not always equal to T_N, being sometimes higher. While the field variation of T_N has been systematically studied in many heavy-fermion systems, that of T_χ^{max}, when it differs from T_N, has generally not been characterized carefully. The question is whether T_χ^{max} vanishes at the same field H_c than T_N or if it vanishes at a field H_m higher than H_c. Recently, a study of $Ce(Ru_{0.92}Rh_{0.08})_2Si_2$ [96] permitted to show the decoupling between the field instabilities at $\mu_0 H_c = 3$ T and $\mu_0 H_m = 6$ T (cf. Fig. 9). In the magnetic field–temperature plane, $H_c(T \to 0)$ is clearly identified as the prolongation of the Néel line $T_N(H)$, and H_m is the prolongation of a crossover line T_α^{max} determined by thermal expansion [89,96], which reaches 6.5 K at zero field and is related to $T_\chi^{max} \simeq 5$ K [Fig. 9(c)]. In the parent compound $CeRu_2Si_2$, $\mu_0 H_m = 8$ T is the prolongation of a crossover line $T_\alpha^{max} \simeq T_\chi^{max} \simeq 10$ K [26,45,46]. The antiferromagnet $Ce(Ru_{0.92}Rh_{0.08})_2Si_2$ has thus both the characteristics of the above-mentioned heavy-fermion antiferromagnets, where H_c scales with T_N, and that of the heavy-fermion paramagnets described in Section 2.1, where H_m scales with T_χ^{max}. Microscopically, as well as static antiferromagnetic moments, which develop below T_N, are quenched above H_c, we speculate that strong antiferromagnetic fluctuations, which would develop below T_χ^{max}, would also collapse above H_m. Inelastic neutron scattering experiments are now needed to test this hypothesis.

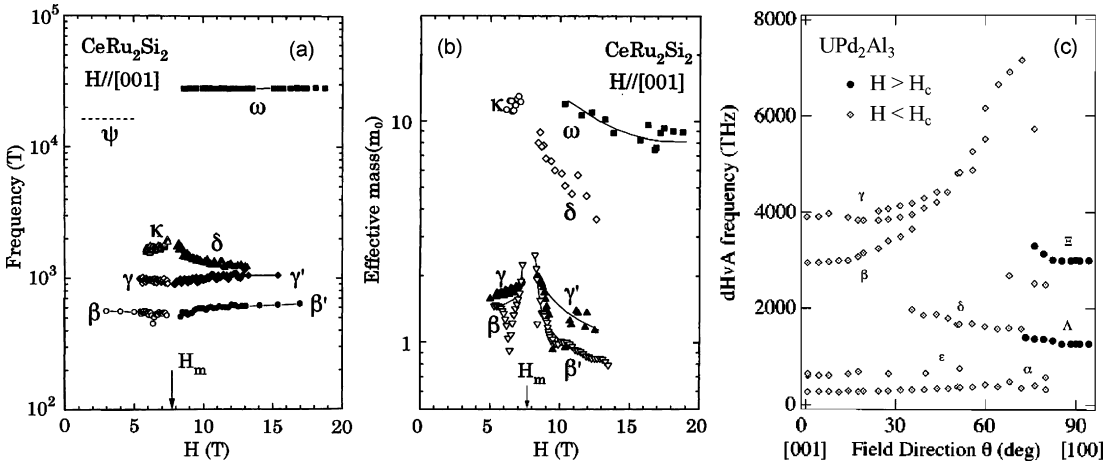

Fig. 10. Modifications of de Haas–van Alphen (a) frequencies and (b) effective masses in the heavy-fermion paramagnet $CeRu_2Si_2$ in a magnetic field applied along **c** [103] (Copyright 1996 The Physical Society of Japan). (c) Angular dependence of de Haas–van Alphen frequencies at magnetic fields below and above the critical field H_c in the heavy-fermion antiferromagnet UPd_2Al_3 [104] (Copyright 1997 The American Physical Society).

2.3. Fermi surface modifications at a field-induced transition

In addition to modifications of the magnetic properties, a sudden change in the Fermi surface has been observed by de Haas–van Alphen oscillations at the magnetic field-induced transitions H_m in the heavy-fermion paramagnet $CeRu_2Si_2$ [103] and H_c in the heavy-fermion antiferromagnet UPd_2Al_3 [104] (see Fig. 10). Controversially, the change of the Fermi surface at H_m in $CeRu_2Si_2$ has been interpreted as the signature of a sudden localization of the f-electrons [103], which is in contradiction with the observation of local (**q**-independent) Kondo magnetic fluctuations above H_m by inelastic neutron scattering [14]. Recent de Haas–van Alphen experiments [51] performed systematically on the whole family $Ce_{1-x}La_xRu_2Si_2$ have also shown a continuous evolution with doping of the Fermi surface in magnetic fields higher than H_m and H_c, which contrasts with the sudden change of the quantum oscillations observed in $CeRu_2Si_2$ when the field is tuned [103]. Another contradiction with the de Haas–van Alphen experiments on $CeRu_2Si_2$ [103] came from Hall effect and magnetoresistivity measurements, which were interpreted as a signature of a continuous evolution of the Fermi surface through H_m [105].

Complementarily to the investigation of the Fermi surface, X-ray absorption spectroscopy is a pertinent tool to determine, via a study of the f-ions valence, how the f-electrons become localized when a magnetic field is applied. This technique has been recently used for the study of valence of the heavy-fermion materials $CeCu_2Si_2$ under pressure up to 8 GPa [106] as well as $YbInCu_4$ [107] and $CeRu_2Si_2$ [108] under a pulsed magnetic field up to 40 T. Knowing that a high-enough magnetic field is expected to quench the Kondo effect, leading to a localization of the f-electrons, X-ray absorption spectroscopy allows to determine whether the magnetic field-induced localization of the f-electrons suddenly occurs at a field-induced transition or progressively develops under magnetic field (with no marked variation at H_c or H_m). Concerning $CeRu_2Si_2$, it has been shown that the f-electron itineracy is progressively suppressed in a high magnetic field applied along **c**, with no Kondo breakdown at $\mu_0 H_m \simeq 8$ T [108].

2.4. The "hidden-order" paramagnet URu_2Si_2

The paramagnet URu_2Si_2 occupies a particular place in the heavy-fermion family. Despite a huge experimental and theoretical effort since more than 20 years [109], the nature of the transition occurring at $T_0 = 17.5$ K and of its associated order parameter is still unknown. Numerous models, as for example that based on antiferromagnetic hexadecapole ordering [110], have been proposed to describe the hidden-order phase below T_0. Enhanced magnetic fluctuations have been reported by inelastic neutron scattering at the wave vectors $\mathbf{Q}_1 = (1.4, 0, 0)$ and $\mathbf{Q}_0 = (1, 0, 0)$ [70] and antiferromagnetic long-range ordering with the wave vector $\mathbf{Q}_0$ is stabilized above a pressure of 0.5 GPa [111]. A magnetic field along the easy magnetic axis **c** destabilizes the hidden-order phase and replaces it, through a cascade of three first-order transitions, by a polarized paramagnetic regime above 39 T [112] [Fig. 11(a)]. The polarized magnetic moment reaches 1.5 μ_B/U at 45 T and continues to increase significantly at higher field [69,114] [Fig. 11(c)], showing that magnetic fluctuations are not fully quenched. Above T_0, the high-field phase diagram looks rather similar to that of usual heavy-fermion paramagnets, as $CeRu_2Si_2$, since the field-induced transition $\mu_0 H_m \simeq 35$–40 T to a polarized regime corresponds to the prolongation in the (T, H) plane of the T_χ^{max} line. As shown in Fig. 11(b), T_χ^{max} decreases with H and vanishes when the field-induced transition to a polarized regime occurs [89]. The correspondence 1 K $\leftrightarrow$ 1 T between T_χ^{max} and H_m, as in many other heavy-fermion paramagnets (Fig. 4), indicates that they are controlled by a single energy scale (Table 1). This scale might be related to antiferromagnet correlations, since $T_\chi^{max} = 55$ K is very close to the antiferromagnetic linewidth $\Gamma(\mathbf{Q}_0, T > T_0) \simeq 50$ K probed by neutron

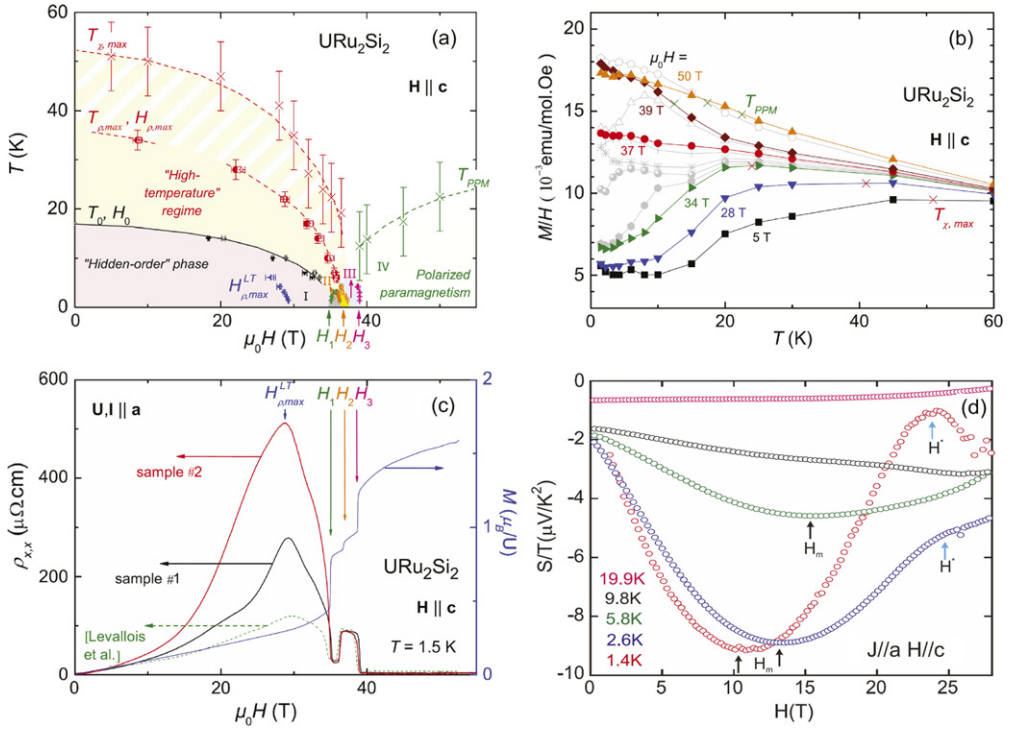

Fig. 11. (a) Magnetic field–temperature phase diagram, (b) magnetization divided by the field versus temperature at different magnetic fields up to 50 T, and (c) magnetoresistance (of three single crystals with different RRR) and magnetization versus field at $T = 1.5$ K [69], and (d) thermoelectric power divided by temperature versus magnetic field at different temperatures up to 27 T, for $\mathbf{H} \parallel \mathbf{c}$ in URu_2Si_2 [113].

scattering above T_0. Similarly to the $CeRu_2Si_2$ case, an extrapolation of neutron data measured up to 17 T is also compatible with a loss above 35 T of antiferromagnetic correlations [90].

The singularity of the compensated metal URu_2Si_2 comes from the strong interplay between its magnetic properties and the properties of its Fermi surface. When entering the "hidden-order" phase below T_0, the Fermi surface is suddenly modified, with a strong reduction of the carrier number and an increase of the carrier mobility [69,115–118]. Below T_0, strong magnetic fluctuations develop at the wave vector $\mathbf{Q}_0$, the linewidth of the magnetic fluctuations at $\mathbf{Q}_0$ and $\mathbf{Q}_1$ has been also significantly reduced [70]. No significant change of the Fermi surface has been seen in the pressure-induced antiferromagnetic state [119], while successive modifications of the Fermi surface were observed when a magnetic field is applied along **c** [120–122], i.e., when substantial magnetic polarization is induced by the magnetic field. Fig. 11(b) shows that the transverse magnetoresistivity $\rho_{x,x}$ measured with $\mathbf{H} \parallel \mathbf{c}$ has a strongly-sample-dependent contribution peaked at 30 T. This anomaly in the orbital contribution to $\rho_{x,x}$ is the signature of a progressive evolution from a high-mobility Fermi surface below 30 T to a low-mobility Fermi surface above 30 T. A broad anomaly in the thermoelectric power at $\mu_0 H^* = 24$ T, as shown in Fig. 11(d), has also been attributed to a Lifshitz transition inside the hidden-order phase [113]. In a high magnetic field applied along **c**, the fact that $T_\chi^{\max}/T_0$ is almost constant indicates that the destabilization of $T_\chi^{\max}$ at 35–39 T drives the destabilization of T_0 and that $T_\chi^{\max}$ is a precursor of T_0. The unique cascade of three first-order transitions occurring in URu_2Si_2 between 35 and 39 T is also a low-temperature consequence – of unknown origin – of the field-induced vanishing of $T_\chi^{\max}$.

3. Field and spin-orientation dependence of the effective mass

The dHvA effect has been successfully applied to numerous strongly correlated electron systems. In some heavy-fermion compounds, dHvA measurements have identified quasiparticles with masses of up to 100 times the bare electron mass [123], thus providing a direct evidence of a huge quasiparticle density of states at the Fermi level, as is suggested by the strongly enhanced linear coefficient of the specific heat, γ. In many of the strongly correlated electron systems to which the dHvA technique has been applied [124], good agreement is found between γ and the measured quasiparticle masses. There are notable exceptions, however, [103,125] where the measured quasiparticle masses add up to significantly less than the measured linear specific heat coefficient. Exotic theories of heavy-fermion behavior invoking neutral fermionic quasiparticles have been proposed to explain the "missing" mass in these systems [126–128]. Another theoretical approach is the possibility of a spin-split Fermi surface with an undetected heavy spin component. The latter possibility received support from measurements by Harrison et al. above the metamagnetic transition in CeB_6 [129], which suggested that quasiparticles of only a single spin orientation were contributing to the dHvA signal.

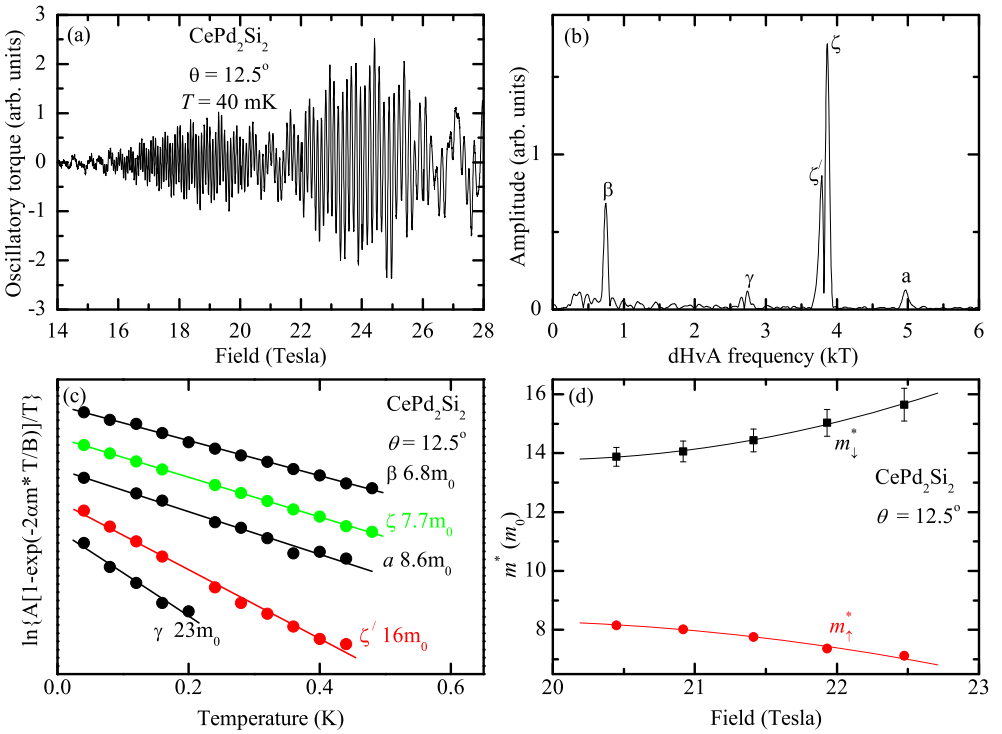

Fig. 12. dHvA oscillatory signal (a) and its Fourier spectrum (b) observed in $CePd_2Si_2$ with magnetic field applied at 12.5° from [100] to [110] direction. Note the splitting of the ζ-frequency. (c) Mass plot for the same orientation of the magnetic field. The slope of the lines allows for the determination of the effective mass, which is found here to vary from 6.8 to 23 m_0. Note the two times difference between the effective masses of the spin-split frequencies ζ and ζ'. (d) Field dependence of both spin-up and spin-down cyclotron effective masses. Lines are guide for the eye only illustrating the monotonic behavior of the effective masses of both spin-split bands above 20 T.

It is well known that in ferromagnetic metals, the band structure calculations usually predict very different majority- and minority-spin Fermi surfaces. The effective masses corresponding to the up- and down-spin orientations are, therefore, also very different. In other materials, however, for a spin-splitting, two sheets of the Fermi surface with opposite orientation of the spins usually have similar shapes and topologies, and thus close values of the effective mass. From this point of view, heavy-fermion compounds represent a remarkable exception. Indeed, modern theories of heavy fermions [130–133] predict different masses and their field dependence for majority and minority carriers. This is supposed to be a fundamental feature of heavy fermions with antiferromagnetic or even non-magnetic ground state.

Experimentally, the magnetic field dependence of the effective mass in heavy fermions was first observed in CeB_6 in 1987. Joss et al. [134] performed low-temperature dHvA measurements in CeB_6 in fields up to 25 T. The authors observed a strong decrease of the quasiparticle effective mass with magnetic field. However, the spin-orientation dependence of the effective mass was not observed. At about the same time, Bredl [135] reported that the low-temperature specific heat coefficient of CeB_6 also decreases with field up to 8 T.

From the experimental point of view, it is often difficult to follow the field dependence of the spin-split effective masses. Small field intervals required for the field dependence are usually not sufficient to resolve the spin-splitting. Sometimes, the splitting cannot be resolved directly even over large field intervals. In this case, an attempt to extract the field dependence of the effective mass by moving a small field window through a large field range produces strange artificial results. A waveform analysis is then a more appropriate technique as will be discussed below. Sometimes, however, the moving window method allows one to extract the field dependence of the effective mass of both spin components.

Below, we will show two examples of heavy-fermion compounds, antiferromagnetic $CePd_2Si_2$ and non-magnetic $CeCoIn_5$, where the spin-splitting of the Fermi surface can be directly resolved in dHvA measurements and the effective masses of both spin components can be extracted and followed as a function of magnetic field. The results presented below were obtained from magnetic torque measurements, in which magnetic field should be applied away from the main crystallographic symmetry axes.

3.1. $CePd_2Si_2$

Figs. 12(a) and (b) show the dHvA signal and the corresponding Fourier spectrum in $CePd_2Si_2$ with magnetic field applied in the basal plane at 12.5° from [100] direction. One of the fundamental peaks is split into two satellites ζ and ζ' with frequencies 3.87 and 3.79 kT respectively. Such a small splitting can be resolved only when analyzing the data over a large

inverse field range. The two close satellites originate from the spin-splitting of the Fermi surface into up- and down-spin bands.

In $CePd_2Si_2$, the effective mass corresponding to the ζ'-peak, 16 m_0, is more than two times higher than that of the other satellite. This can be seen unambiguously in Fig. 12(c) showing the mass plot. Such a remarkable difference would be surprising in other metals, but is rather expected in heavy-fermion compounds, where different masses are predicted theoretically for up- and down-spin bands. A similar behavior has been observed in $PrPb_3$ [136], where the effective masses of up- and down-spin oscillations were found to be very different, up to a factor of two, although the frequencies were also very close to each other. Such a big difference in the effective masses might shed some light on the puzzling situation in some other f-electron compounds, e.g. CeB_6 [129,137], where the oscillations from only one spin state were observed. Indeed, this would be the case if the other spin channel had too large effective mass to be detected.

Direct observation of the splitting of the ζ-frequency (Fig. 12(b)) provides an opportunity to trace the field dependence of the effective mass of both spin components. The field dependence of both up- and down-spin effective masses of the ζ-orbit is shown in Fig. 12(d). The analysis was limited to fields above 20 T, where the splitting of the ζ-orbit could be resolved unambiguously. The effective mass of the spin-down band increases continuously with increasing field and that of the spin-down band shows a monotonic decrease. This behavior is in good qualitative agreement with modern theoretical models [130–133]. An extension of these measurements to higher fields is required to check whether the effective masses of both spin components still depend on field monotonically above 28 T.

3.2. $CeCoIn_5$

Previous moderate field dHvA studies of $CeCoIn_5$ [138,139] have revealed essentially all the Fermi surface sheets predicted by theoretical band structure calculations performed for itinerant f-electron. The thermodynamics is dominated by two large, quasi-2D sheets, α and β. Strongly enhanced effective masses up to 87 m_0 were found to be field-dependent.

More recently, the quasiparticle masses of the thermodynamically important α and β sheets of the Fermi surface were studied in more details by McCollam et al. [140]. The authors analyzed temperature dependence of the dHvA oscillations over the field range of 13 to 15 T and down to very low temperature of 6 mK. They demonstrated that the conventional Lifshitz–Kosevich formula fails to provide a satisfactory fit of the data. However, when spin-dependent effective masses were taken into account, the modified "spin-dependent" Lifshitz–Kosevich theory provided an excellent fit. It should be emphasized, however, that McCollam et al. have not observed the spin-splitting of the oscillatory signal directly. The spin-split effective masses were extracted from the analysis of the temperature dependence of the oscillatory signal of a single frequency.

Our dHvA measurements in $CeCoIn_5$ were performed at field up to 28 T and temperature down to 40 mK. While the base temperature of our experiment was not nearly as low as that of McCollam et al. [140], a larger inverse field range of our measurements resulted in a much better dHvA frequency resolution. The oscillatory signal obtained with magnetic field applied at 2.5° from c- to a-axis at $T = 40$ mK is shown in Fig. 13(a). The corresponding Fourier transform for a field range from 15 to 28 T is shown in Fig. 13(b). The splitting of the α_1-frequency is quite clear without any further analysis. The values of the split frequencies, 5.42 and 5.49 kT, are very close to each other and differ by only about 1%. It is not surprising, therefore, that the splitting could not be resolved in previous measurements over a much smaller inverse field range.

At a first glance, the α_2 peak does not appear to be split. Its broadening and characteristic asymmetric shape, however, indicate that it consists of two very close peaks. This can be seen in the inset of Fig. 13(b) showing a zoom of the frequencies originating from the α sheet of the Fermi surface. Indeed, an attempt to fit the α_2 peak with a double-peak Gaussian function (the red line) produces an excellent result and reveals two close satellites (the green lines). The frequencies of the satellites, 4.80 and 4.85 kT, also differ by about 1%.

Fig. 13(c) shows the mass plot of the split frequencies α_1 and α_2 from Fig. 13(b). The spin-dependent effective masses of the α_1 orbit, 11.1 ± 0.3 m_0 and 16.3 ± 0.4 m_0, differ by about 50%. However, the difference between the effective masses of the α_2 satellites, α_{21} and α_{22}, 23.4 ± 1.3 m_0 and 9.9 ± 0.3 m_0 is more than a factor of two. This ratio is similar to that observed in $CePd_2Si_2$ as discussed above. The ratio of the two masses is also similar to that found by McCollam et al. [140] for the α_3 orbit at 13–15 T.

The field dependence of the effective masses corresponding to both up- and down-spin bands of the α_1-orbit is shown in Fig. 13(d). Contrary to $CePd_2Si_2$, here both the up-spin and down-spin effective masses vary monotonically with field. However, surprisingly, both masses are found to decrease with increasing field. The effective mass of the spin-up band decreases faster, changing by 21% from 19 to 21 T. The effective mass of the spin-down band varies by 12% over the same field range.

The decrease of both spin components masses with magnetic field observed here agrees with the results of McCollam et al. [140] who reported the same behavior, although their results were obtained at much lower fields. At a first glance, this behavior seems to be at odds with the existing modern theories, as all of them predict an increase of one of the spin-dependent masses and a decrease of the other one. However, very recently it was shown [141] that in ferromagnetic state of heavy-fermion compounds, the application of sufficiently strong magnetic field leads to a full polarization of the system. Then both spin-up and spin-down masses decrease with increasing magnetic field. This might explain the unusual

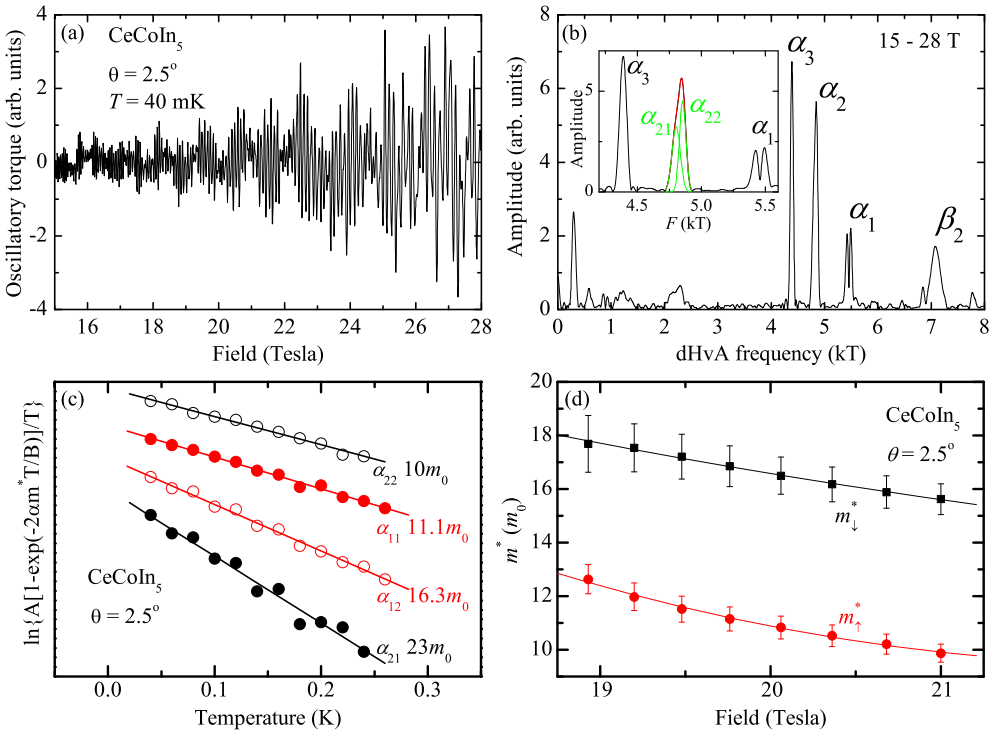

Fig. 13. dHvA oscillatory signal (a) and its Fourier spectrum from 15 to 28 T (b) observed in $CeCoIn_5$ with magnetic field applied at 2.5° from [100] to [001] direction. The spin-splitting of the α_1 and β_2 frequencies can be seen clearly. The inset zooms on the frequencies originating from the α sheet of the Fermi surface. The characteristic shape and broadening of the α_2 peak implies that it is composed of two close satellites. The satellites (green lines) are indeed revealed by fitting the peak by a two-peak Gaussian function (red line). (c) Mass plot for the spin-split frequencies α_1 (red) and α_2 (black) for the same orientation of the magnetic field. Open and close symbols correspond to the different spin components. (d) Effective masses of both spin components of the α_1-orbit as a function of applied field. Lines are guide for the eye. (For interpretation of the references to color in this figure legend, the reader is referred to the web version of this article.)

behavior of the effective masses observed here, even though $CeCoIn_5$ is non-magnetic at zero magnetic field. However, neutron diffraction measurements have never been performed at high magnetic field.

4. Non-centrosymmetric compounds

Non-centrosymmetric heavy-fermion compounds have recently attracted a lot of experimental and theoretical interest. The absence of inversion symmetry in the crystal lattice and a strong spin–orbit coupling in these materials lead to the splitting of the electronic energy bands. The Fermi surface of such a metal is, therefore, also split into two surfaces characterized by different chirality as schematically shown in Fig. 14. This naturally results in the appearance of two distinct frequencies in the spectra of dHvA oscillations. It was demonstrated theoretically [142] that the analysis of the oscillatory spectra in such materials provides a direct measure of the strength of the spin–orbit coupling. It is thus very important to obtain detailed and precise dHvA frequencies and their angular dependence in materials without inversion center.

Here, we illustrate the experimental observation of the Fermi surface splitting by dHvA measurements in non-centrosymmetric $CeCoGe_3$ performed in field up to 28 T. The dHvA effect in $CeCoGe_3$ was previously investigated in magnet fields up to 17 T [143]. Four fundamental frequencies were identified, all of them split due to spin–orbit interaction. The frequencies themselves and their angular dependencies are in a rather good agreement with the results of theoretical band structure calculations performed for $LaCoGe_3$, implying localized f-electrons. As compared to other non-centrosymmetric compounds, the splitting of dHvA frequencies in $CeCoGe_3$ is relatively small, indicating a moderate spin–orbit coupling of about 100 K. The highest effective mass observed in $CeCoGe_3$ is 12 bare electron masses corresponding to the β-branch. Finally, only one frequency originating from the α-branch representing the biggest Fermi surface was initially observed in $CeCoGe_3$.

The dHvA oscillations observed in $CeCoGe_3$ between 20 and 28 T are shown in Fig. 15(a). All the fundamental frequencies previously observed in $CeCoGe_3$ are still present at high field (Fig. 15(b)). In addition, both components of the α-branch are now clearly resolved. With magnetic field applied at 9° from the crystallographic c-axis, the two frequencies are close to each other, $F_{\alpha^+} = 10.17$ kT and $F_{\alpha^-} = 10.47$ kT. The most significant and surprising result, however, is the presence of the new fundamental frequencies, A and B, in the Fourier spectrum of $CeCoGe_3$. The new frequencies, $F_A = 12.31$ kT and $F_B = 19.42$ kT are considerably higher than the highest frequency, F_α, reported for lower fields.

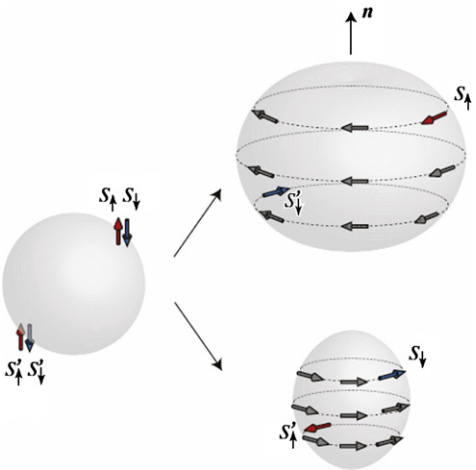

Fig. 14. Schematic illustration of the Fermi surface splitting in non-centrosymmetric materials. The original Fermi surface (in the left) is split into two surfaces characterized by different chirality (in the right).

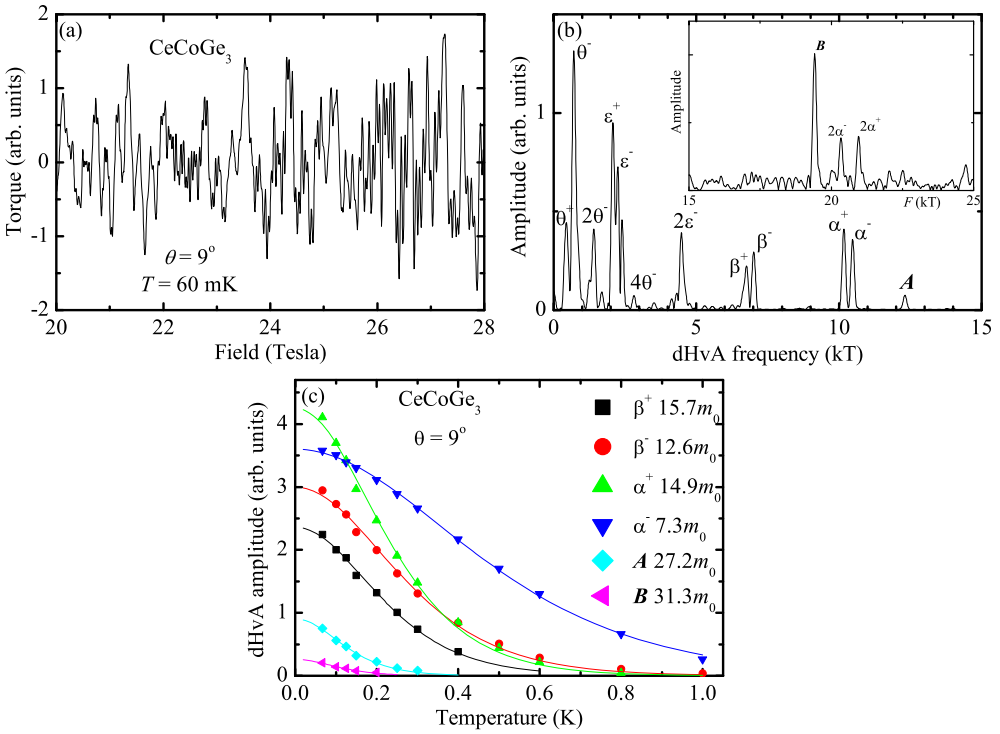

Fig. 15. dHvA oscillatory signal (a) and its Fourier spectrum (b) observed in $CeCoGe_3$ with magnetic field (20–28 T) applied at 9° from [100] to [110] at $T = 60$ mK. The frequencies denoted by θ, ϵ, β and α were observed in the previous lower-field measurements (with the exception of α^+-branch). The frequencies denoted by A and B are observed only at high field and were not detected in the previous measurements. (c) Temperature dependence of the dHvA amplitude is shown for α- and β-branches as well as for the new frequencies A and B. Lines are the fits to the temperature-dependent part of the Lifshitz–Kosevich formula. The effective masses, m^*, obtained from the fits are also shown.

Fig. 15(c) shows the temperature dependence of the dHvA amplitudes of the new frequencies A and B as well as α- and β-branches in $CeCoGe_3$ for magnetic field applied at 9° from the crystallographic c-axis. These data allow one to determine effective masses by fitting the experimental points to the temperature-dependent part of the Lifshitz–Kosevich formula. The best fits to the formula along with the extracted effective masses are also shown in Fig. 15(c). It was previously reported [143] that α- and β-branches possess the highest effective masses of 8 and 12 bare electron masses respectively. These values are very close to the current results if only the α^- frequency is considered and taking into account that only a single frequency from the α-branch was initially observed in the previous measurements. Interestingly, the effective masses of the two frequencies originating from the α-branch differ by a factor of more than two, being 14.9 and 7.3 bare electron

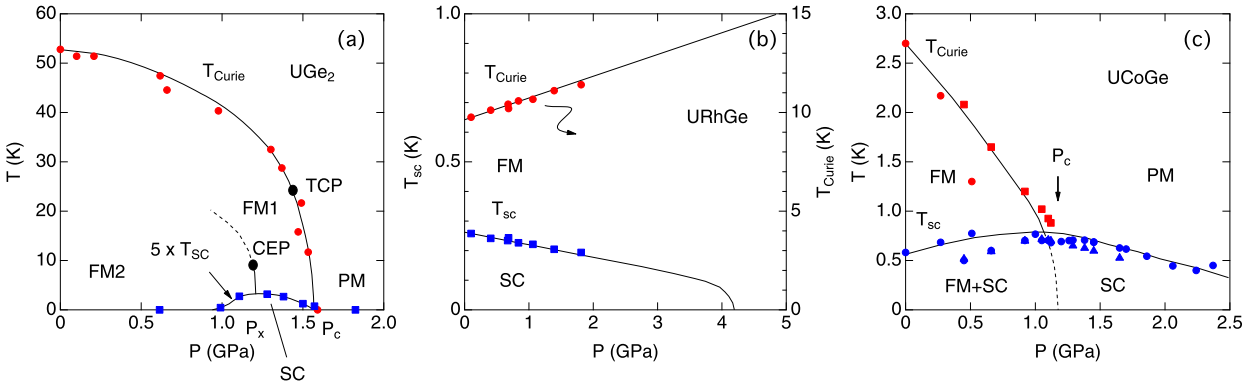

Fig. 16. (T, P) phase diagram of (a) UGe_2, (b) URhGe and (c) UCoGe [21,148–152].

masses for α^+ and α^- frequencies respectively. This is in contrast with all the other branches where the effective masses of the two components are quite close to each other. The most surprising result, however, is that the effective masses of the new frequencies are strongly enhanced being 27 m_0 and 31 m_0 for A and B respectively. These values by far exceed the masses of the other previously observed frequencies.

For the moment, it is not clear where the two new high dHvA frequencies observed and $CeCoGe_3$ originate from. Neither of them was detected in the previous lower-field measurements or revealed by theoretical band structure calculations. The frequencies correspond to strongly enhanced effective masses implying that they represent thermodynamically important parts of the Fermi surface. While it is not certain if the frequencies appear in high magnetic field only or simply experimentally undetectable at lower field, they certainly do not originate from magnetic breakdown. They are, therefore, likely to be intrinsic and are possibly due to a field-induced modification of the Fermi surface, especially as similar new frequencies were also detected in the non-4f analog $LaCoGe_3$ [144]. It would be interesting to see if new frequencies emerge in other non-centrosymmetric compounds at high field.

5. U-based ferromagnetic superconductors

Ferromagnetism (FM) and superconductivity (SC) are usually antagonistic, because the strong internal field due to ferromagnetism generally easily destroys superconductivity. In the early 1980s extensive studies had been done for the exceptional cases of several materials, such as Chevrel phase compounds ($REMo_6Se_8$, RE: rare earth) and $ErRh_4B_4$, where the magnetic moment is relatively large and SC phase is expelled when the FM state is established [145]. In this case, the Curie temperature (T_{Curie}) is lower than the superconducting critical temperature (T_{sc}). In the special cases where the SC coherence length ξ is larger than the size of magnetic domain d, SC can coexist with FM in a narrow temperature range. At lower temperatures, SC is destroyed, which illustrates that SC and FM compete with each other.

The microscopic coexistence of FM and SC was theoretically predicted for the well-known weak ferromagnet $ZrZn_2$ [146], where a spin-triplet state with equal spin pairing was expected to be formed near the ferromagnetic quantum critical point. However, there are no experimental evidences for SC in this material, although extrinsic SC due to Zr-alloys on the surface was reported [147].

The first discovery of coexistence of FM and SC was reported in UGe_2 [21], where SC is observed only in the FM phase just below the critical pressure at which FM is suppressed. URhGe is the first ferromagnet which shows SC already at ambient pressure [22]. T_{Curie} (= 9.5 K) is much higher than T_{sc} (= 0.25 K), indicating that the SC phase exists in the FM phase. Coexistence of SC and FM is also found in UCoGe [24], which has the same crystal structure than URhGe. The weak ferromagnet UIr also shows SC just below the critical pressure of ferromagnetism [23]. The (T, P) phase diagram with multiple FM phases is more complicated, and bulk SC properties, for example in the specific heat, have not been confirmed yet. Here we do not describe the details of UIr further.

All the known materials where FM coexists microscopically with SC are uranium compounds with substantially reduced magnetic moments compared to the free ion values. The 5f-electrons in these systems have in general an intermediate nature between itinerant 3d-electrons and localized 4f-electrons. The magnetic moment of uranium compounds varies from nearly free ion values (localized case) to the very tiny values (itinerant case). Furthermore, a strong spin–orbit interaction also plays an important role for the physical properties. The ferromagnetic superconductors mentioned above have relatively small magnetic moments, thus 5f-electrons in these compounds are thought to be itinerant at first approximation.

5.1. UGe_2 and the ferromagnetic quantum critical end point

Fig. 16(a) shows the (T, P) phase diagram of UGe_2 [21,148,149]. The large T_{Curie} at ambient pressure in UGe_2 is suppressed by applying pressure. At the critical pressure $P_c \sim 1.5$ GPa, FM completely collapses and a paramagnetic (PM) ground state is realized. SC is observed only in the FM regime just below P_c. The maximum of T_{sc} is found at $P_x \sim 1.2$ GPa,

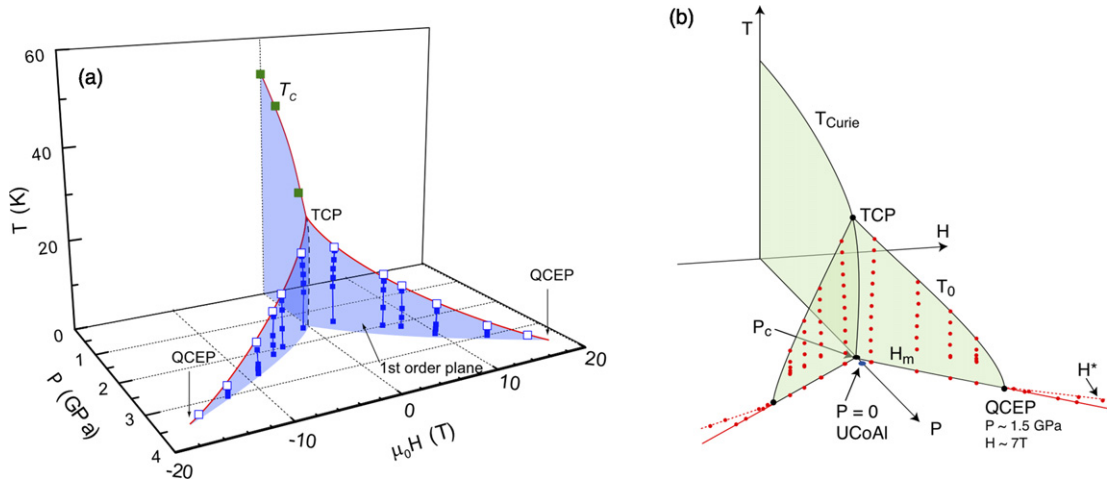

Fig. 17. (T, P, H) phase diagram of (a) UGe_2 [153,154] and (b) UCoAl [155].

where T_x collapses. FM below T_{Curie} consists of two phases FM1 and FM2, which are separated by T_x. The phase FM1 between T_{Curie} and T_x is weakly polarized ($M_0 \sim 1\ \mu_B$), while the phase FM2 below T_x is strongly polarized ($M_0 \sim 1.5\ \mu_B$). At low pressure the boundary between FM1 and FM2 is a crossover, and at the pressure P_{CEP} (just below P_x) it changes into a first-order transition, at a point called critical end point (CEP). T_{Curie} also changes into a first-order transition at the tri-critical point (TCP) at P_{TCP}, which is just below P_c.

When the magnetic field is applied along the a-axis (easy-magnetization axis) at $P > P_c$, the phase FM1 is recovered from the low-field PM phase through a sharp first-order metamagnetic transition. At $P_x < P < P_c$, a step-like first-order metamagnetic transition from FM1 to FM2 is also observed. The (T, P, H) phase diagram of UGe_2 is shown in Fig. 17(a). The critical temperature decreases with field from the TCP defined at zero field and terminates at the quantum critical end point (QCEP, at $P_{\text{QCEP}} \sim 3.5$ GPa, $H_{\text{QCEP}} \sim 18$ T). By crossing the first-order plane (between the TCP and the QCEP, for T below the critical temperature), we can observe a sharp metamagnetic transition. A similar "wing"-shaped phase diagram is also realized between FM1 and FM2, however the critical field at which the first-order transition terminates is probably much higher.

De Haas–van Alphen (dHvA) experiments clearly demonstrate that the Fermi surfaces in FM1, FM2 and in the PM phase are quite different [156,157]. For example, for $H \parallel b$, dHvA branches present in FM2 disappear in FM1, while completely new dHvA branches appear in the PM phase. Agreement between these experiments with the results of band calculations is not clear, because of the low symmetry of the crystal structure and the large polarized moment. Nevertheless, a cylindrical shape of the Fermi surfaces is expected due to the flat Brillouin zone along the a-axis. The cyclotron effective mass gradually increases with pressure. In the PM phase, a large mass ranging from 20 to 60 m_0 is detected, which is consistent with the pressure variation of the Sommerfeld coefficient γ detected from specific heat measurements [158].

In itinerant ferromagnets or nearly ferromagnets, a metamagnetic transition from PM to field-induced FM can occur. The well-known materials are the weak ferromagnet $ZrZn_2$ [159] and the nearly ferromagnetic compound $Sr_3Ru_2O_7$ [43]. In particular, $Sr_3Ru_2O_7$ has attracted a strong interest following the finding of a new quantum phase called "nematic" phase [160]. A difficulty to investigate the QCEP in UGe_2 is to combine high magnetic field and high pressure, which prevents from a detailed study of ferromagnetic quantum criticality. A new system which can be easily tuned to the ferromagnetic quantum criticality has been recently found: UCoAl [155]. As shown in Fig. 17(b), the ground state of UCoAl is PM, and a first-order metamagnetic transition from PM to FM is observed at low field for $H \parallel c$. By applying pressure, the metamagnetic transition field H_m increases, and its first-order nature terminates at $P_{\text{QCEP}} \sim 1.5$ GPa and $H_{\text{QCEP}} \sim 7$ T, where a sharp enhancement of the effective mass is detected by resistivity measurements. An interesting point is that the first-order metamagnetic transition changes into a second-order transition or crossover above the QCEP, and a new phase appears between H_m and H^*, with a plateau in the resistivity coefficient A and residual resistivity ρ_0 (see Fig. 18). More detailed studies focusing on the Fermi surface instabilities are now required.

Evidences for the coexistence of FM and SC in UGe_2 were obtained by neutron diffraction [149] and NQR experiments [161]. Bulk SC was confirmed by specific heat measurements, as shown in Fig. 19(a) [158]. An interesting point is that a large residual γ-term remains at 0 K. For comparison, the specific heat results in URhGe and UCoGe are also shown in Figs. 19(b), (c) [22,162]. Even for high-quality samples, as confirmed by their high residual resistivity ratio (RRR), the residual γ-values (γ_0) are large, implying that a larger ordered moment yields a larger residual γ-value (see Fig. 20). A possible reason might be that one of the spin components for the equal spin pairing is not gapped ($\Delta_{\downarrow\downarrow} \approx 0$), and the other spin components are only gapped ($\Delta_{\uparrow\uparrow} \neq 0$) and are responsible for the development of SC. Another possible reason might be that the materials are always in an SC mixed state (with no lower critical field H_{c1}), because of a large internal

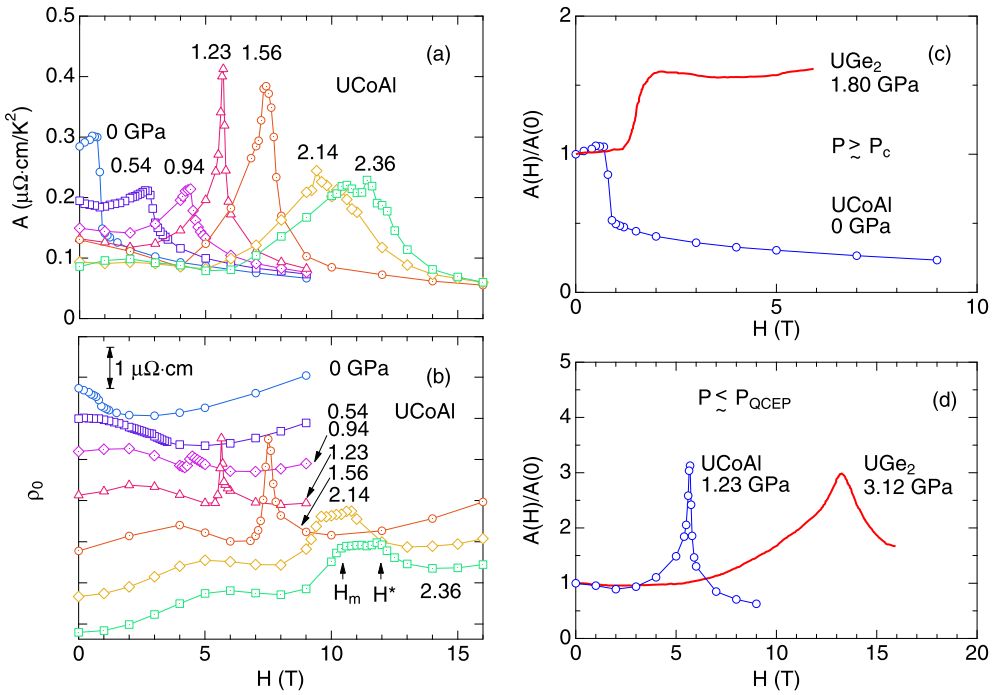

Fig. 18. Field dependence of the resistivity coefficient A (a) and residual resistivity ρ_0 (b) at various pressures in UCoAl. A comparison with the coefficient A of UGe_2 is shown in panels (c) and (d) [155].

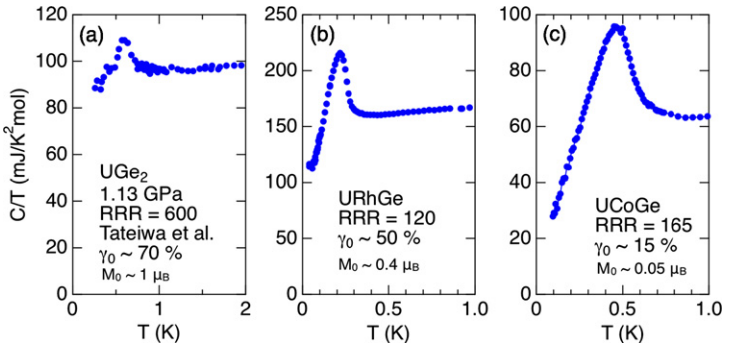

Fig. 19. Specific heat at low temperatures in (a) UGe_2, (b) URhGe and (c) UCoGe [22,158,162].

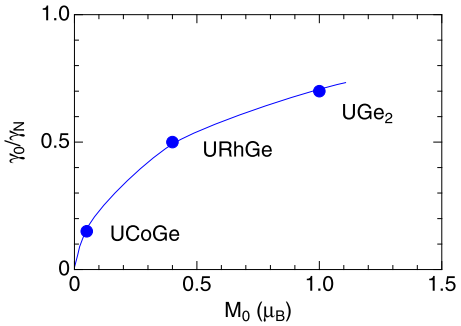

Fig. 20. Residual γ-value as a function of the ordered moment.

field proportional to the ordered moment. To confirm the residual γ-values as an intrinsic origin, systematic specific heat experiments on samples of different qualities are required.

When the pressure is tuned between P_x and P_c, the upper critical field H_{c2} for $H \parallel a$ shows a peculiar temperature dependence, as shown in Fig. 21(a) [163]. The S-shaped curve of H_{c2} is connected to the boundary between the two

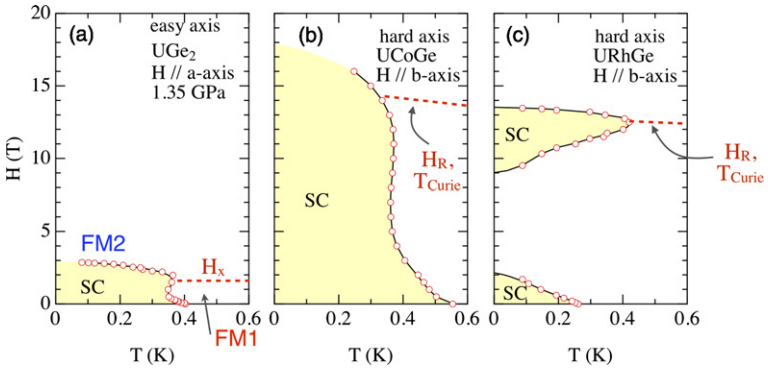

Fig. 21. H_{c2} curves of (a) UGe_2, (b) UCoGe and (c) URhGe.

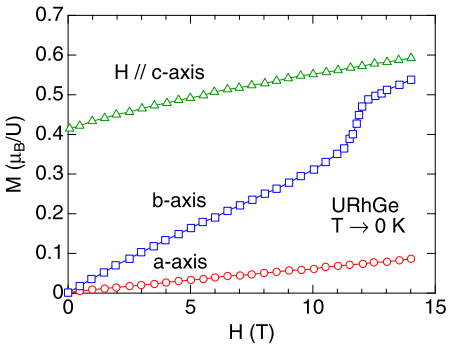

Fig. 22. Magnetization curves of URhGe [165].

different ferromagnetic states FM1 and FM2. The Fermi surface instabilities associated with the enhancement of the effective mass reinforce the SC phase. The value of $H_{c2}(0)$ is much higher than the Pauli limit expected for the weak coupling BCS scheme. Thus, it is natural that the spin-triplet state with equal spin paring is realized, where SC persists even in a large ferromagnetic exchange field.

5.2. Huge and anisotropic H_{c2} in URhGe and UCoGe

URhGe shows SC at $T_{sc} = 0.25$ K already at ambient pressure [22]. T_{Curie} ($= 9.5$ K) is much higher than T_{sc}, and the moment is directed along the c-axis in the TiNiSi-type orthorhombic structure. The ordered moment is 0.4 μ_B which is considerably reduced from the free ion value, 3.6 μ_B, for both $5f^2$ and $5f^3$ configurations. The large specific heat γ-value 160 mJ/K^2 mol indicates that URhGe is a heavy-fermion compound. By applying pressure, T_{Curie} increases while T_{sc} decreases, indicating that pressure drives URhGe away from its critical region [see Fig. 16(b)], which can be also inferred from thermal expansion measurements via applying the Ehrenfest relation [150,151,164].

Fig. 22 shows the magnetization M versus field H curves extrapolated to 0 K for a magnetic field applied along the a-, b- and c-axes [165]. The initial slope of $M(H)$ for $H \parallel b$ is large compared to that for H along the easy-magnetization c-axis, indicating that the moment starts to tilt from c- to b-axis, which finally ends by a spin reorientation occurring at $H_R \approx 12$ T, where the moment is completely directed along the hard-magnetization b-axis.

Surprisingly, field-reentrant superconductivity is found just below H_R for $H \parallel b$ [16]. As shown in Fig. 21(c), SC is first destroyed at 2 T but, in further increasing field, SC reappears in the field range from 8 to 13 T. It should be noted that the critical temperature of SC at 12 T is higher than that at zero field, meaning that SC is indeed reinforced under magnetic field. Since the reentrant SC dome at high fields is connected to the spin reorientation, it is natural to consider that the ferromagnetic fluctuations associated with the spin reorientation induce SC. If the field direction is slightly tilted from b- to c-axis, the reentrant SC phase is immediately suppressed [166]. On the other hand, when the field direction is tilted from b- to a-axis, the reentrant SC phase shifts to the higher field range, following the $1/\cos\theta$ dependence of H_R (θ: field angle from b- to a-axis) [17].

Similar field-reinforced SC is also found in UCoGe [167]. The crystal structure of UCoGe is identical to that of URhGe. In UCoGe, T_{Curie} is equal to 2.5 K and SC is observed at 0.6 K at ambient pressure [24]. As shown in Fig. 16(c), T_{Curie} decreases with increasing pressure and reaches zero at $P_c \sim 1$ GPa, while T_{sc} increases, shows a maximum at P_c, and then decreases, indicating that SC survives even in the PM phase [152,168]. This phase diagram is quite different from that obtained in UGe_2 and also from theoretical predictions that T_{sc} should drop at P_c.

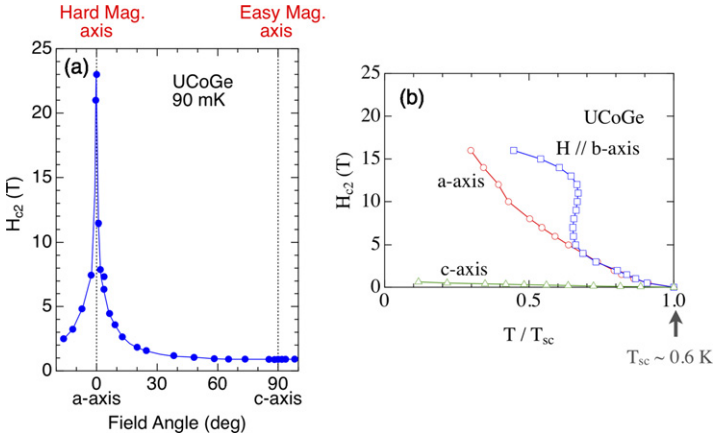

Fig. 23. (a) Angular dependence of H_{c2} at 90 mK for $H \parallel a \rightarrow c$, and (b) temperature dependence of H_{c2} for $H \parallel a$, b and c [167].

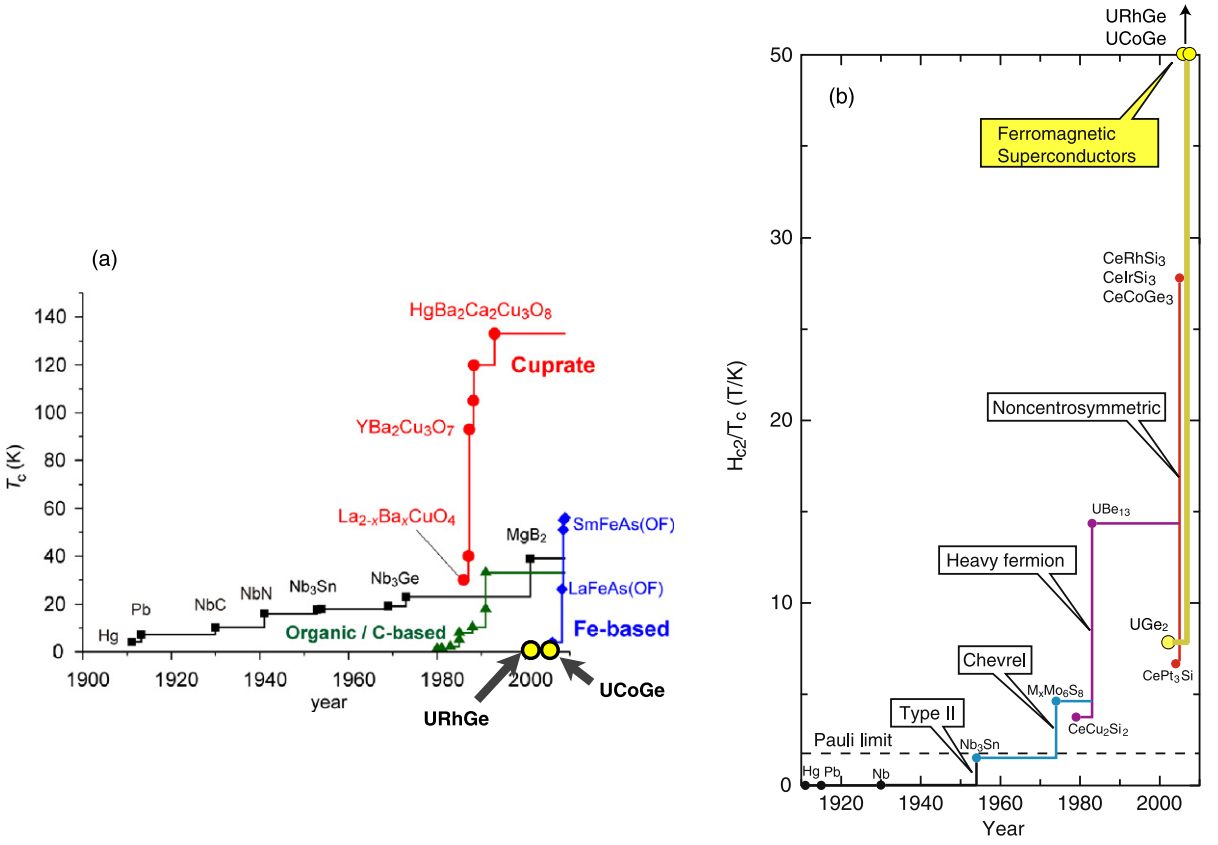

Fig. 24. History of T_{sc} and H_{c2}/T_{sc} [169,170].

H_{c2} in UCoGe is quite anisotropic. As shown in Fig. 23, H_{c2} for $H \parallel c$ is rather small, since it equals ~ 1 T, which is close to the Pauli limit. However, when the field is applied along the hard-magnetization a- and b-axes, a huge H_{c2} is observed [167]. For $H \parallel a$, the H_{c2} curve shows an unusual upward curvature, H_{c2} probably reaching more than 25 T at 0 K. For $H \parallel b$, an unusual H_{c2} curve with an "S"-shape is further observed, H_{c2} at 0 K being also huge (~ 20 T). When the field is slightly tilted to the easy-magnetization c-axis, H_{c2} at low temperature is strongly suppressed as shown in Fig. 23. The values of $H_{c2}(0)$ for $H \parallel a$ and b greatly exceed the Pauli limit, indicating that a spin-triplet state with equal-spin pairing is responsible for SC.

Fig. 24(a) shows that the highest superconducting temperature has been strongly enhanced since 100 years [169], from conventional to unconventional superconductors, including the recently discovered new class of U-based superconductors. Fig. 24(b) shows the evolution with time of H_{c2} divided by T_{sc} for various superconductors [170]. In general H_{c2} is governed

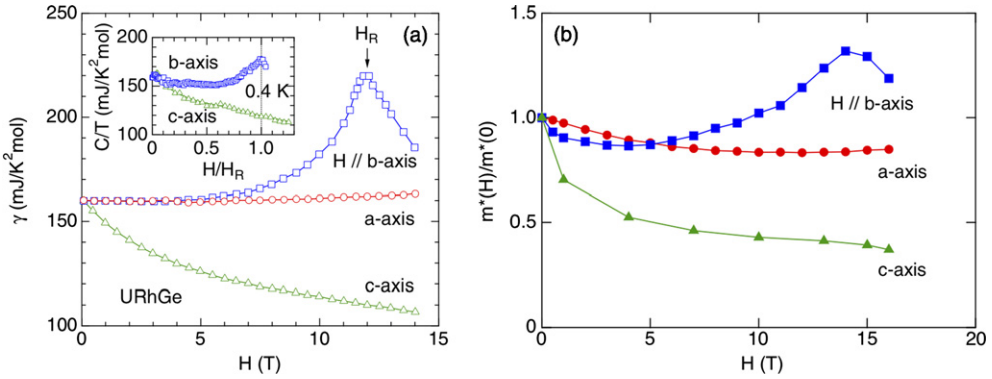

Fig. 25. (a) Field dependence of the specific heat γ-value for $H \parallel a$, b and c in URhGe [165] and (b) field dependence of the resistivity coefficient A in UCoGe [167]. The data in the main panel of (a) were obtained from the temperature dependence of the magnetization using the Maxwell relation. The inset in (a) shows direct specific heat measurements.

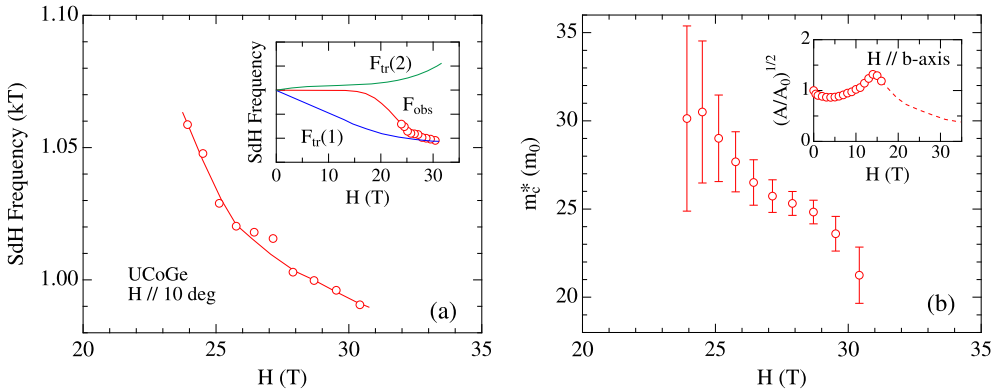

Fig. 26. (a) Field dependence of the SdH frequency at high field in UCoGe and (b) the field dependence of the cyclotron effective mass.

either by the Pauli limit or by the orbital limit. In conventional BCS superconductors, the initial slope of $H_{c2}(T)$ at $H = 0$ is small and H_{c2} at 0 K is also small. In heavy-fermion superconductors, the initial slope is potentially large because of the large effective mass. H_{c2} is, however, limited by the Pauli limit due to the Zeeman splitting based on the spin-singlet state. In the case of no Pauli paramagnetic effect due to a spin-triplet state, H_{c2} would be only governed by the orbital limit. Thus, a huge H_{c2} is expected in heavy-fermion compounds, where the orbital limit can be described as $\Psi_0/2\pi\xi^2$ or $0.73\,\mathrm{d}H_{c2}/\mathrm{d}T\,T_{sc}$ within the clean limit. This is indeed realized in non-centrosymmetric compounds and ferromagnetic superconductors.

As shown in Fig. 25, the field response of the specific heat γ-value is anisotropic both in URhGe and in UCoGe [165–167,171]. The γ-value for $H \parallel c$ decreases with increasing field, as expected for usual weak ferromagnets where the spin fluctuations are suppressed under magnetic field. Oppositely, for $H \parallel b$ γ shows a maximum at the field where the field-reinforced SC (or RSC) is observed, indicating that ferromagnetic fluctuations are enhanced. For $H \parallel a$, the γ-value retains a large value, but a maximum is not observed.

In the simple model proposed in Ref. [171], the superconducting temperature can be written as $T_{sc} \sim \exp(-m^*/m^{**})$, where the effective mass m^* can be approximated by $m^* = (1+\lambda)m_B \equiv m_B + m^{**}$, where m_B is the band mass and m^{**} is an extra mass directly related to the SC pairing. If the extra mass (correlation mass) m^{**} is enhanced, T_{sc} is also enhanced. Furthermore, as H_{c2} is governed by the orbital limit ($\sim \Psi_0/2\pi\xi^2$), H_{c2} can be simply described as $H_{c2} \propto (m^* T_{sc})^2$, using the relations $\xi \sim \hbar v_F/k_B T_{sc}$ and $m^* v_F = \hbar k_F$. Therefore, if the effective mass is enhanced, a large H_{c2} accompanied with the increased T_{sc} can be expected. In fact, anomalous phenomena, such as the "S"-shaped H_{c2} curve in UCoGe and the field-reentrant SC phase of URhGe where $T_{sc}(H_R)$ is larger than $T_{sc}(0)$, can be naturally explained. It is worth noting that here we simply assume invariant Fermi surfaces under magnetic field.

An interesting question is whether the Fermi surface is really unchanged near the field-reinforced SC region. In UCoGe, Shubnikov–de Haas (SdH) experiments [172] show that the observed SdH frequency (~ 1 kT) decreases with increasing field just above H_{c2} (see Fig. 26), indicating a non-linear field response of the Zeeman-split Fermi surface. Correspondingly, the cyclotron mass also decreases with increasing field. A shrinkage of the Fermi surface near RSC was reported from SdH experiments in URhGe [173]. Since the Fermi surfaces observed in these experiments carry only 12% and 1.5% of the total specific heat γ-value in UCoGe and URhGe, respectively, a definite conclusion is still under debate. It should be noted

that recent high-field thermopower measurements on UCoGe show a sharp peak around 11 T for $H \parallel b$, suggesting the modification of the Fermi surface [174].

In summary of this section, high-field experiments have revealed a new aspect of ferromagnetic quantum critical phenomena and field-reinforced SC in ferromagnetic superconductors. The Ising-type longitudinal ferromagnetic fluctuations play an important role for the anisotropic and huge H_{c2}, as it has been clarified by NMR experiments on UCoGe [175]. On the other hand, it has been recently proposed that XY-type transverse magnetic fluctuations might lead to raise T_{sc} in AF or nearly AF compounds [176]. Precise experiments with microscopic experimental probes, such as NMR, neutron scattering and quantum oscillations, are required for the future studies.

Acknowledgements

We acknowledge G. Ballon, F. Bourdarot, D. Braithwaite, J.P. Brison, A. Buzdin, T. Combier, A. Demuer, J. Flouquet, S. Fujimoto, K. Goetze, P. Haen, F. Hardy, H. Harima, K. Hasselbach, E. Hassinger, T. Hattori, L. Howald, A. Huxley, D. Hykel, K. Ishida, N. Kimura, G. Knebel, H. Kotegawa, G. Lapertot, P. Lejay, F. Lévy, L. Malone, T.D. Matsuda, C. Meingast, V. Michal, V. Mineev, A. Miyake, K. Miyake, Y. Ōnuki, C. Paulsen, C. Proust, S. Raymond, G. Scheerer, R. Settai, J. Spalek, Y. Tada, V. Taufour, D. Vignolle, A. de Visser, S. Watanabe, J. Wosnitza, H. Yamagami, and E. Yelland. This work was supported by the French ANR DELICE, by Euromagnet II via the EU under Contract No. RII3-CT-2004-506239, and by the ERC Starting Grant NewHeavyFermion.

References

[1] J. Flouquet, On the heavy fermion road, Prog. Low Temp. Phys. 15 (2005) 139–281.
[2] Hilbert v. Löhneysen, Achim Rosch, Matthias Vojta, Peter Wölfle, Fermi-liquid instabilities at magnetic quantum phase transitions, Rev. Modern Phys. 79 (Aug 2007) 1015–1075.
[3] S. Doniach, The Kondo lattice and weak antiferromagnetism, Physica B+C 91 (1977) 231–234.
[4] J.R. Iglesias, C. Lacroix, B. Coqblin, Revisited Doniach diagram: Influence of short-range antiferromagnetic correlations in the Kondo lattice, Phys. Rev. B 56 (18) (Nov 1997) 11820–11826.
[5] G.R. Stewart, Non-Fermi-liquid behavior in d- and f-electron metals, Rev. Modern Phys. 73 (4) (Oct 2001) 797–855.
[6] Christian Pfleiderer, Superconducting phases of f-electron compounds, Rev. Modern Phys. 81 (4) (Nov 2009) 1551–1624.
[7] Tôru Moriya, Tetsuya Takimoto, Anomalous properties around magnetic instability in heavy electron systems, J. Phys. Soc. Jpn. 64 (3) (1995) 960–969.
[8] John A. Hertz, Quantum critical phenomena, Phys. Rev. B 14 (3) (Aug 1976) 1165–1184.
[9] A.J. Millis, Effect of a nonzero temperature on quantum critical points in itinerant fermion systems, Phys. Rev. B 48 (10) (Sept 1993) 7183–7196.
[10] P. Coleman, C. Pépin, Qimiao Si, R. Ramazashvili, How do Fermi liquids get heavy and die?, J. Phys., Condens. Matter 13 (35) (2001) R723–R738.
[11] W. Knafo, S. Raymond, P. Lejay, J. Flouquet, Antiferromagnetic criticality at a heavy-fermion quantum phase transition, Nature Phys. 5 (10) (Oct 2009) 753–757.
[12] J. Custers, P. Gegenwart, H. Wilhelm, K. Neumaier, Y. Tokiwa, O. Trovarelli, C. Geibel, F. Steglich, C. Pepin, P. Coleman, The break-up of heavy electrons at a quantum critical point, Nature 424 (6948) (July 2003) 524–527.
[13] Masugu Sato, Yoshihiro Koike, Susumu Katano, Naoto Metoki, Hiroaki Kadowaki, Shuzo Kawarazaki, Field-induced ferromagnetic correlation in the heavy-fermion compound $CeRu_2Si_2$, J. Phys. Soc. Jpn. 70 (Supplement A) (2001) 118.
[14] S. Raymond, D. Raoelison, S. Kambe, L.P. Regnault, B. Fåk, R. Calemczuk, J. Flouquet, P. Haen, P. Lejay, Magnetic instabilities in $CeRu_2Si_2$ compounds, Phys. B: Condens. Matter 259–261 (1999) 48–53.
[15] J. Flouquet, Y. Haga, P. Haen, D. Braithwaite, G. Knebel, S. Raymond, S. Kambe, Phase diagram of heavy fermion systems, in: Proceedings of the International Conference on Magnetism (ICM 2003), J. Magn. Magn. Mater. 272–276 (Part 1) (2004) 27–31.
[16] F. Levy, I. Sheikin, B. Grenier, A.D. Huxley, Magnetic field-induced superconductivity in the ferromagnet URhGe, Science 309 (5739) (2005) 1343–1346.
[17] F. Levy, I. Sheikin, B. Grenier, A.D. Huxley, Acute enhancement of the upper critical field for superconductivity approaching a quantum critical point in URhGe, Nature Phys. 3 (2007) 460–463.
[18] E. Bauer, G. Hilscher, H. Michor, Ch. Paul, E.W. Scheidt, A. Gribanov, Yu. Seropegin, H. Noël, M. Sigrist, P. Rogl, Heavy fermion superconductivity and magnetic order in noncentrosymmetric $CePt_3Si$, Phys. Rev. Lett. 92 (Jan 2004) 027003.
[19] V.M. Edel'shtein, Characteristics of the Cooper pairing in two-dimensional noncentrosymmetric electron systems, Sov. Phys. JETP 68 (6) (June 1989) 1244–1249.
[20] Lev P. Gor'kov, Emmanuel I. Rashba, Superconducting 2D system with lifted spin degeneracy: Mixed singlet-triplet state, Phys. Rev. Lett. 87 (July 2001) 037004.
[21] S.S. Saxena, P. Agarwal, K. Ahilan, F.M. Grosche, R.K.W. Haselwimmer, M.J. Steiner, E. Pugh, I.R. Walker, S.R. Julian, P. Monthoux, G.G. Lonzarich, A. Huxley, I. Sheikin, D. Braithwaite, J. Flouquet, Superconductivity on the border of itinerant-electron ferromagnetism in UGe_2, Nature 406 (6796) (2000) 587–592.
[22] Dai Aoki, Andrew Huxley, Eric Ressouche, Daniel Braithwaite, Jacques Flouquet, Jean-Pascal Brison, Elsa Lhotel, Carley Paulsen, Coexistence of superconductivity and ferromagnetism in URhGe, Nature 413 (6856) (2001) 613–615.
[23] T. Akazawa, H. Hidaka, T. Fujiwara, T.C. Kobayashi, E. Yamamoto, Y. Haga, R. Settai, Y. Ōnuki, Pressure-induced superconductivity in ferromagnetic UIr without inversion symmetry, J. Phys., Condens. Matter 16 (4) (2004) L29.
[24] N.T. Huy, A. Gasparini, D.E. de Nijs, Y. Huang, J.C.P. Klaasse, T. Gortenmulder, A. de Visser, A. Hamann, T. Görlach, H. v. Löhneysen, Superconductivity on the border of weak itinerant ferromagnetism in UCoGe, Phys. Rev. Lett. 99 (6) (Aug 2007) 067006.
[25] P. Haen, J. Flouquet, F. Lapierre, P. Lejay, G. Remenyi, Metamagnetic-like transition in $CeRu_2Si_2$?, J. Low Temp. Phys. 67 (1987) 391–419.
[26] J. Flouquet, P. Haen, S. Raymond, D. Aoki, G. Knebel, Itinerant metamagnetism of $CeRu_2Si_2$: bringing out the dead. Comparison with the new $Sr_3Ru_2O_7$ case, Physica B 319 (1–4) (2002) 251–261.
[27] A. Schröder, H.G. Schlager, H. v. Löhneysen, Magnetization of $CeCu_6$ at low temperatures, J. Magn. Magn. Mater. 108 (1992) 47–48.
[28] H. v. Löhneysen, H.G. Schlager, A. Schröder, Magnetic correlations and magnetic ordering in $CeCu_{6-x}Au_x$ single crystals, Physica B 186 (188) (1993) 590–592.
[29] W. Knafo, D. Aoki, D. Vignolles, B. Vignolle, Y. Klein, C. Jaudet, A. Villaume, C. Proust, J. Flouquet, High-field metamagnetism in the antiferromagnet $CeRh_2Si_2$, Phys. Rev. B 81 (9) (Mar 2010) 094403.

[30] I. Sheikin, A. Gröger, S. Raymond, D. Jaccard, D. Aoki, H. Harima, J. Flouquet, High magnetic field study of $CePd_2Si_2$, Phys. Rev. B 67 (9) (Mar 2003) 094420.

[31] Y. Tokiwa, P. Gegenwart, F. Weickert, R. Küchler, J. Custers, J. Ferstl, C. Geibel, F. Steglich, Suppression of the Kondo state in $YbRh_2Si_2$ by large magnetic fields, J. Magn. Magn. Mater. 272–276 (2004) E87–E88.

[32] E. Stryjewski, N. Giordano, Metamagnetism, Adv. Phys. 26 (5) (1977) 487–650.

[33] T. Sakakibara, T. Goto, K. Yoshimura, K. Murata, K. Fukamichi, Susceptibility maximum and metamagnetism in nearly ferromagnetic Laves phase intermetallic compounds, J. Magn. Magn. Mater. 90–91 (1990) 131–134.

[34] T. Sakakibara, T. Goto, K. Yoshimura, K. Fukamichi, Itinerant electron metamagnetism and spin fluctuations in nearly ferromagnetic metals $Y(Co_{1-x}Al_x)_2$, J. Phys., Condens. Matter 2 (14) (1990) 3381.

[35] T. Inoue, K. Kindo, H. Okuni, K. Sugiyama, Y. Haga, E. Yamamoto, T.C. Kobayashi, Y. Uwatoko, Y. Onuki, High-field magnetization of URu_2Si_2 under high pressure, in: Proceedings of the Sixth International Symposium on Research in High Magnetic Fields, Phys. B: Condens. Matter 294–295 (2001) 271–275.

[36] Tadashi Fukuhara, Kunihiko Maezawa, Hitoshi Ohkuni, Junji Sakurai, Hideyuki Sato, Hisashi Azuma, Kiyohiro Sugiyama, Yoshichika Ōnuki, Koichi Kindo, Metamagnetic behavior of the heavy-fermion compound $CeNi_2Ge_2$, J. Phys. Soc. Jpn. 65 (6) (1996) 1559–1561.

[37] Kiyohiro Sugiyama, Tomoya Iizuka, Dai Aoki, Yoshifumi Tokiwa, Kousaku Miyake, Narumi Watanabe, Koichi Kindo, Tetsutaro Inoue, Etsuji Yamamoto, Yoshinori Haga, Yoshichika Ōnuki, High-field magnetization of USn_3 and UPb_3, J. Phys. Soc. Jpn. 71 (1) (2002) 326–331.

[38] Yoshichika Ōnuki, Rikio Settai, Kiyohiro Sugiyama, Tetsuya Takeuchi, Tatsuo C. Kobayashi, Yoshinori Haga, Etsuji Yamamoto, Recent advances in the magnetism and superconductivity of heavy fermion systems, J. Phys. Soc. Jpn. 73 (4) (2004) 769–787.

[39] Tetsuya Takeuchi, Shinichi Yasui, Masatoshi Toda, Masaki Matsushita, Shingo Yoshiuchi, Masahiro Ohya, Keisuke Katayama, Yusuke Hirose, Naohisa Yoshitani, Fuminori Honda, Kiyohiro Sugiyama, Masayuki Hagiwara, Koichi Kindo, Etsuji Yamamoto, Yoshinori Haga, Toshiki Tanaka, Yasunori Kubo, Rikio Settai, Yoshichika Ōnuki, Metamagnetic behavior in heavy-fermion compound $YbIr_2Zn_{20}$, J. Phys. Soc. Jpn. 79 (6) (2010) 064609.

[40] M.T. Béal-Monod, Field effects in strongly enhanced paramagnets, in: 16th International Conference on Low Temperature Physics, Physica B+C 109–110 (Part 3) (1982) 1837–1848.

[41] Rikio Settai, Tetsuya Takeuchi, Yoshichika Ōnuki, Recent advances in Ce-based heavy-fermion superconductivity and Fermi surface properties, J. Phys. Soc. Jpn. 76 (5) (2007) 051003.

[42] A.J. Millis, A.J. Schofield, G.G. Lonzarich, S.A. Grigera, Metamagnetic quantum criticality in metals, Phys. Rev. Lett. 88 (21) (May 2002) 217204.

[43] S.A. Grigera, R.S. Perry, A.J. Schofield, M. Chiao, S.R. Julian, G.G. Lonzarich, S.I. Ikeda, Y. Maeno, A.J. Millis, A.P. Mackenzie, Magnetic field-tuned quantum criticality in the metallic ruthenate $Sr_3Ru_2O_7$, Science 294 (5541) (2001) 329–332.

[44] S.A. Grigera, P. Gegenwart, R.A. Borzi, F. Weickert, A.J. Schofield, R.S. Perry, T. Tayama, T. Sakakibara, Y. Maeno, A.G. Green, A.P. Mackenzie, Disorder-sensitive phase formation linked to metamagnetic quantum criticality, Science 306 (5699) (2004) 1154–1157.

[45] R.A. Fisher, C. Marcenat, N.E. Phillips, P. Haen, F. Lapierre, P. Lejay, J. Flouquet, J. Voiron, The magnetic instability in the heavy fermion compounds $Ce_{1-x}La_xRu_2Si_2$, J. Low Temp. Phys. 84 (1991) 49–86.

[46] C. Paulsen, A. Lacerda, L. Puech, P. Haen, P. Lejay, J.L. Tholence, J. Flouquet, A. Visser, Low-temperature properties of the heavy-fermion compound $CeRu_2Si_2$ at the metamagnetic transition, J. Low Temp. Phys. 81 (1990) 317–339.

[47] Stéphane Raymond, William Knafo, Jacques Flouquet, Pascal Lejay, Further analysis of the quantum critical point of $Ce_{1-x}La_xRu_2Si_2$, J. Low Temp. Phys. 147 (2007) 215–230.

[48] J.-M. Mignot, J. Flouquet, P. Haen, F. Lapierre, L. Puech, J. Voiron, Metamagnetic $CeRu_2Si_2$: New perspectives for heavy-fermion studies in high fields, J. Magn. Magn. Mater. 76–77 (1988) 97–104.

[49] J.G. Park, P. Haen, P. Lejay, J. Voiron, Non-linear susceptibility in heavy fermion compounds $CeRu_2Si_2$ and $Ce_{1-x}Y_xRu_2Si_2$ ($x <$ or $= 0.1$), J. Phys., Condens. Matter 6 (44) (1994) 9383.

[50] P. Haen, A. de Visser, F. Lapierre, Concentration dependence of the pseudometamagnetic field in heavy fermion $Ce_{1-x}Y_xRu_2Si_2$, in: Research in High Magnetic Fields, Phys. B: Condens. Matter 211 (1–4) (1995) 230–232.

[51] Yuji Matsumoto, Motoki Sugi, Noriaki Kimura, Takemi Komatsubara, Haruyoshi Aoki, Isamu Satoh, Taichi Terashima, Shinya Uji, Continuous evolution of Fermi surface properties above metamagnetic transitions in $Ce_xLa_{1-x}Ru_2Si_2$, J. Phys. Soc. Jpn. 77 (5) (2008) 053703.

[52] Yuji Matsumoto, Noriaki Kimura, Haruyoshi Aoki, Motoi Kimata, Taichi Terashima, Shinya Uji, Tetsuo Okane, Hiroshi Yamagami, Delocalization of the f electron in $Ce_xLa_{1-x}Ru_2Si_2$, J. Phys. Soc. Jpn. 79 (8) (2010) 083706.

[53] W. Knafo, S. Raymond, J. Flouquet, B. Fåk, M.A. Adams, P. Haen, F. Lapierre, S. Yates, P. Lejay, Anomalous scaling behavior of the dynamical spin susceptibility of $Ce_{0.925}La_{0.075}Ru_2Si_2$, Phys. Rev. B 70 (Nov 2004) 174401.

[54] Yuji Matsumoto, Motoki Sugi, Kosuke Aoki, Yasunobu Shimizu, Noriaki Kimura, Takemi Komatsubara, Haruyoshi Aoki, Motoi Kimata, Taichi Terashima, Shinya Uji, Magnetic phase diagram and Fermi surface properties of $CeRu_2(Si_{1-x}Ge_x)_2$, J. Phys. Soc. Jpn. 80 (7) (2011) 074715.

[55] Hitoshi Sugawara, Yuji Aoki, Hideyuki Sato, Nikolay Mushnikov, Tsuneaki Goto, New heavy fermion metamagnet $CeFe_2Ge_2$, J. Phys. Soc. Jpn. 68 (4) (1999) 1094–1097.

[56] T. Ebihara, K. Motoki, H. Toshima, M. Takashita, N. Kimura, H. Sugawara, K. Ichihashi, R. Settai, Y. Onuki, Y. Aoki, H. Sato, Magnetic properties of single crystal $CeFe_2Ge_2$, in: Proceedings of the International Conference on Strongly Correlated Electron Systems, Phys. B: Condens. Matter 206–207 (1995) 219–221.

[57] B. Fåk, J. Flouquet, G. Lapertot, T. Fukuhara, H. Kadowaki, Magnetic correlations in single-crystalline $CeNi_2Ge_2$, J. Phys., Condens. Matter 12 (25) (2000) 5423.

[58] E.C. Palm, T.P. Murphy, Donavan Hall, S.W. Tozer, R.G. Goodrich, J.L. Sarrao, Magnetic transitions in $CeIrIn_5$, in: Proceedings of the 23rd International Conference on Low Temperature Physics, Phys. B: Condens. Matter 329–333 (Part 2) (2003) 587–588.

[59] Tetsuya Takeuchi, Tetsutaro Inoue, Kiyohiro Sugiyama, Dai Aoki, Yoshihumi Tokiwa, Yoshinori Haga, Koichi Kindo, Yoshichika Ōnuki, Magnetic and thermal properties of $CeIrIn_5$ and $CeRhIn_5$, J. Phys. Soc. Jpn. 70 (3) (2001) 877–883.

[60] T. Willers, Z. Hu, N. Hollmann, P.O. Körner, J. Gegner, T. Burnus, H. Fujiwara, A. Tanaka, D. Schmitz, H.H. Hsieh, H.-J. Lin, C.T. Chen, E.D. Bauer, J.L. Sarrao, E. Goremychkin, M. Koza, L.H. Tjeng, A. Severing, Crystal-field and Kondo-scale investigations of $CeMIn_5$ ($M =$ Co, Ir, and Rh): A combined x-ray absorption and inelastic neutron scattering study, Phys. Rev. B 81 (May 2010) 195114.

[61] J. Rossat-Mignod, L.P. Regnault, J.L. Jacoud, C. Vettier, P. Lejay, J. Flouquet, E. Walker, D. Jaccard, A. Amato, Inelastic neutron scattering study of cerium heavy fermion compounds, J. Magn. Magn. Mater. 76–77 (1988) 376–384.

[62] M. Deppe, S. Lausberg, F. Weickert, M. Brando, Y. Skourski, N. Caroca-Canales, C. Geibel, F. Steglich, Pronounced first-order metamagnetic transition in the paramagnetic heavy-fermion system CeTiGe, Phys. Rev. B 85 (Feb 2012) 060401.

[63] S. Kitagawa, H. Ikeda, Y. Nakai, T. Hattori, K. Ishida, Y. Kamihara, M. Hirano, H. Hosono, Metamagnetic behavior and Kondo breakdown in heavy-fermion CeFePO, Phys. Rev. Lett. 107 (Dec 2011) 277002.

[64] Yusuke Hirose, Masatoshi Toda, Shingo Yoshiuchi, Shinichi Yasui, Kiyohiro Sugiyama, Fuminori Honda, Masayuki Hagiwara, Koichi Kindo, Rikio Settai, Yoshichika Ōnuki, Metamagnetic transition in heavy fermion compounds YbT_2Zn_{20} (T: Co, Rh, Ir), J. Phys. Conf. Ser. 273 (1) (2011) 012003.

[65] Tetsuya Takeuchi, Masahiro Ohya, Shingo Yoshiuchi, Masaki Matsushita, Fuminori Honda, Rikio Settai, Yoshichika Ōnuki, Metamagnetic behavior in a heavy fermion compound $YbCo_2Zn_{20}$, J. Phys. Conf. Ser. 273 (1) (2011) 012059.

[66] J.L. Sarrao, C.D. Immer, Z. Fisk, C.H. Booth, E. Figueroa, J.M. Lawrence, R. Modler, A.L. Cornelius, M.F. Hundley, G.H. Kwei, J.D. Thompson, F. Bridges, Physical properties of YbXCu$_4$ (X = Ag, Au, Cd, Mg, Tl, and Zn) compounds, Phys. Rev. B 59 (Mar 1999) 6855–6866.

[67] N. Tsujii, H. Mitamura, T. Goto, K. Yoshimura, K. Kosuge, T. Terashima, T. Takamasu, H. Kitazawa, S. Kato, G. Kido, High-field properties of the heavy-fermion system $YbCu_5$ and related intermetallics, in: Proceedings of the Sixth International Symposium on Research in High Magnetic Fields, Phys. B: Condens. Matter 294–295 (2001) 284–287.

[68] M. Loewenhaupt, C.-K. Loong, Magnetic excitations in USn_3, Phys. Rev. B 41 (May 1990) 9294–9300.

[69] G.W. Scheerer, W. Knafo, D. Aoki, G. Ballon, A. Mari, D. Vignolles, J. Flouquet, Interplay of magnetism, Fermi surface reconstructions, and hidden order in the heavy-fermion material URu_2Si_2, Phys. Rev. B 85 (Mar 2012) 094402.

[70] C. Broholm, H. Lin, P.T. Matthews, T.E. Mason, W.J.L. Buyers, M.F. Collins, A.A. Menovsky, J.A. Mydosh, J.K. Kjems, Magnetic excitations in the heavy-fermion superconductor URu_2Si_2, Phys. Rev. B 43 (June 1991) 12809–12822.

[71] K. Sugiyama, M. Nakashima, D. Aoki, K. Kindo, N. Kimura, H. Aoki, T. Komatsubara, S. Uji, Y. Haga, E. Yamamoto, H. Harima, Y. Ōnuki, Metamagnetic transition in UPt_3 studied by high-field magnetization and de Haas–van Alphen experiments, Phys. Rev. B 60 (Oct 1999) 9248–9251.

[72] V.T. Rajan, J.H. Lowenstein, N. Andrei, Thermodynamics of the Kondo model, Phys. Rev. Lett. 49 (Aug 1982) 497–500.

[73] V.T. Rajan, Magnetic susceptibility and specific heat of the Coqblin–Schrieffer model, Phys. Rev. Lett. 51 (July 1983) 308–311.

[74] E.P. Wohlfarth, P. Rhodes, Collective electron metamagnetism, Philos. Mag. 7 (83) (1962) 1817–1824.

[75] S.M.M. Evans, Theory of the metamagnetic transition in heavy-fermion compounds, Europhys. Lett. 17 (5) (1992) 469.

[76] H. Yamada, Metamagnetic transition and susceptibility maximum in an itinerant-electron system, Phys. Rev. B 47 (May 1993) 11211–11219.

[77] Katsurou Hanzawa, Keiichi Ohara, Kei Yosida, Magnetization in heavy-fermion compounds, J. Phys. Soc. Jpn. 66 (10) (1997) 3001–3004.

[78] Yoshiaki Ōno, Theory of metamagnetism in the heavy fermion compound $CeRu_2Si_2$, J. Phys. Soc. Jpn. 67 (7) (1998) 2197–2200.

[79] R. Konno, The theory of the magnetization process in $CeRu_2Si_2$, J. Phys., Condens. Matter 3 (49) (1991) 9915.

[80] Yoshinori Takahashi, Tôru Sakai, Theory of itinerant-electron metamagnetism: II. The origin of the susceptibility maximum, J. Phys., Condens. Matter 10 (24) (1998) 5373.

[81] Hiroyuki Satoh, Fusayoshi J. Ohkawa, Field-induced ferromagnetic exchange interaction in metamagnetic transitions of heavy-electron liquids, Phys. Rev. B 57 (Mar 1998) 5891–5899.

[82] A. Lacerda, A. de Visser, P. Haen, P. Lejay, J. Flouquet, Thermal properties of heavy-fermion $CeRu_2S_2$, Phys. Rev. B 40 (Nov 1989) 8759–8768.

[83] Hiroaki Kadowaki, Masugu Sato, Shuzo Kawarazaki, Spin fluctuation in heavy fermion $CeRu_2Si_2$, Phys. Rev. Lett. 92 (Mar 2004) 097204.

[84] S. Quezel, P. Burlet, J.L. Jacoud, L.P. Regnault, J. Rossat-Mignod, C. Vettier, P. Lejay, J. Flouquet, Magnetic ordering in $Ce_xLa_{1-x}Ru_2Si_2$ solid solutions, J. Magn. Magn. Mater. 76–77 (1988) 403–404.

[85] P. Haen, T. Fukuhara, Study of the crossover from ferromagnetic to antiferromagnetic ground state in $CeRu_2(Ge_{0.7}Si_{0.3})_2$ by resistivity measurements under pressure, in: The International Conference on Strongly Correlated Electron Systems, Phys. B: Condens. Matter 312–313 (2002) 437–439.

[86] J.-M. Mignot, L.-P. Regnault, J.-L. Jacoud, J. Rossat-Mignod, P. Haen, P. Lejay, Incommensurabilities and metamagnetism in the heavy-fermion alloys $(Ce_{0.8}La_{0.2})Ru_2Si_2$ and $CeRu_2(Si_{0.9}Ge_{0.1})_2$, Phys. B: Condens. Matter 171 (1–4) (1991) 357–361.

[87] Kenji Watanabe, Yoshiya Uwatoko, Yoshikazu Tabata, Hiroaki Kadowaki, Chikahide Kanadani, Toshifumi Taniguchi, Shuzo Kawarazaki, Pressure-induced instability of magnetic order in Kondo-lattice system: Neutron diffraction study of the pseudo-binary alloy system $Ce(Ru_{0.90}Rh_{0.10})_2(Si_{1-y}Ge_y)_2$, J. Phys. Soc. Jpn. 72 (7) (2003) 1751–1757.

[88] K. Ishida, Y. Kawasaki, Y. Kitaoka, K. Asayama, H. Nakamura, J. Flouquet, Ru NMR and NQR probes of the metamagnetic transition in $CeRu_2Si_2$, Phys. Rev. B 57 (May 1998) R11054–R11057.

[89] When H_m is determined from the magnetization or from its uniaxial pressure derivative, the magnetostriction, versus magnetic field, it corresponds to the change to a high magnetization regime, i.e., to the polarized paramagnetic regime. An increase with the temperature of this characteristic field was reported for $CeRu_2Si_2$ [26], $Ce(Ru_{0.92}Rh_{0.08})_2Si_2$ [96], and URu_2Si_2 [71], confirming that this definition leads to a scale characteristic of the high-field polarized regime. To extract the characteristic scale of the low-field paramagnetic regime, it is appropriate to consider the temperature $T_\chi^{\max}$ at the maximum of the magnetic susceptibility versus temperature, or the temperature $T_\alpha^{\max}$ at the extremum of the thermal expansion versus temperature (cf. [46,88] for $CeRu_2Si_2$ and [69] for URu_2Si_2, where $T_\chi^{\max}$ and $T_\alpha^{\max}$ vanish at H_m)

[90] F. Bourdarot, B. Fåk, K. Habicht, K. Prokeš, Inflection point in the magnetic field dependence of the ordered moment of URu_2Si_2 observed by neutron scattering in fields up to 17 T, Phys. Rev. Lett. 90 (Feb 2003) 067203.

[91] Takuo Sakon, Noriaki K. Sato, Yoshiki Nakanishi, Takemi Komatsubara, Mitsuhiro Motokawa, Magnetic phase diagram of UPd_2Al_3 in high magnetic fields, Jpn. J. Appl. Phys. 41 (Part 1, No. 6A) (2002) 3673–3677.

[92] Rikio Settai, Akira Misawa, Shingo Araki, Masato Kosaki, Kiyohiro Sugiyama, Tetsuya Takeuchi, Koichi Kindo, Yoshinori Haga, Etsuji Yamamoto, Yoshichika Ōnuki, Single crystal growth and magnetic properties of $CeRh_2Si_2$, J. Phys. Soc. Jpn. 66 (8) (1997) 2260–2263.

[93] G. Knebel, R. Boursier, E. Hassinger, G. Lapertot, P.G. Niklowitz, A. Pourret, B. Salce, J.P. Sanchez, I. Sheikin, P. Bonville, H. Harima, J. Flouquet, Localization of $4f$ state in $YbRh_2Si_2$ under magnetic field and high pressure: Comparison with $CeRh_2Si_2$, J. Phys. Soc. Jpn. 75 (11) (2006) 114709.

[94] M.A. Avila, M. Sera, T. Takabatake, $YbNiSi_3$: An antiferromagnetic Kondo lattice with strong exchange interaction, Phys. Rev. B 70 (Sept 2004) 100409.

[95] K. Grube, W. Knafo, S. Drobnik, P. Adelmann, Th. Wolf, C. Meingast, H. v. Löhneysen, Suppression of magnetic order in $CeNiSi_3$ by magnetic fields, in: Proceedings of the 17th International Conference on Magnetism, J. Magn. Magn. Mater. 310 (2, Part 1) (2007) 354–356.

[96] Dai Aoki, Carley Paulsen, Hisashi Kotegawa, Frédéric Hardy, Christoph Meingast, Pierre Haen, Mounir Boukahil, William Knafo, Eric Ressouche, Stephane Raymond, Jacques Flouquet, Decoupling between field-instabilities of antiferromagnetism and pseudo-metamagnetism in Rh-doped $CeRu_2Si_2$ Kondo lattice, J. Phys. Soc. Jpn. 81 (3) (2012) 034711.

[97] D.K. Singh, A. Thamizhavel, J.W. Lynn, S. Dhar, J. Rodriguez-Rivera, T. Herman, Field-induced quantum fluctuations in the heavy fermion superconductor $CeCu_2Ge_2$, Sci. Rep. 1 (Oct 13, 2011).

[98] Takao Ebihara, N. Harrison, M. Jaime, Shinya Uji, J.C. Lashley, Emergent fluctuation hot spots on the Fermi surface of $CeIn_3$ in strong magnetic fields, Phys. Rev. Lett. 93 (Dec 2004) 246401.

[99] A.V. Silhanek, Takao Ebihara, N. Harrison, M. Jaime, Koji Tezuka, V. Fanelli, C.D. Batista, Nonlocal magnetic field-tuned quantum criticality in cubic $CeIn_{3-x}Sn_x$ ($x = 0.25$), Phys. Rev. Lett. 96 (May 2006) 206401.

[100] L.S. Wu, Y. Janssen, C. Marques, M.C. Bennett, M.S. Kim, K. Park, Songxue Chi, J.W. Lynn, G. Lorusso, G. Biasiol, M.C. Aronson, Magnetic field tuning of antiferromagnetic Yb_3Pt_4, Phys. Rev. B 84 (Oct 2011) 134409.

[101] Naoyuki Tateiwa, Shugo Ikeda, Yoshinori Haga, Tatsuma D. Matsuda, Etsuji Yamamoto, Kiyohiro Sugiyama, Masayuki Hagiwara, Koichi Kindo, Yoshichika Ōnuki, Magnetic field and pressure phase diagrams of uranium heavy-fermion compound U_2Zn_{17}, J. Phys. Soc. Jpn. 80 (1) (2011) 014706.

[102] D. Schulze Grachtrup, M. Bleckmann, B. Willenberg, S. Süllow, M. Bartkowiak, Y. Skourski, H. Rakoto, I. Sheikin, J.A. Mydosh, Field-induced phases in UPt_2Si_2, Phys. Rev. B 85 (Feb 2012) 054410.

[103] Masahiro Takashita, Haruyoshi Aoki, Taichi Terashima, Shinya Uji, Kunihiko Maezawa, Rikio Settai, Yoshichika Ōnuki, dHvA effect study of metamagnetic transition in $CeRu_2Si_2$. II – The state above the metamagnetic transition, J. Phys. Soc. Jpn. 65 (2) (1996) 515–524.

[104] T. Terashima, C. Haworth, M. Takashita, H. Aoki, N. Sato, T. Komatsubara, Heavy fermions survive the metamagnetic transition in UPd_2Al_3, Phys. Rev. B 55 (May 1997) R13369–R13372.

[105] R. Daou, C. Bergemann, S.R. Julian, Continuous evolution of the Fermi surface of $CeRu_2Si_2$ across the metamagnetic transition, Phys. Rev. Lett. 96 (2) (2006) 026401.

[106] J.-P. Rueff, S. Raymond, M. Taguchi, M. Sikora, J.-P. Itié, F. Baudelet, D. Braithwaite, G. Knebel, D. Jaccard, Pressure-induced valence crossover in superconducting $CeCu_2Si_2$, Phys. Rev. Lett. 106 (May 2011) 186405.

[107] Y.H. Matsuda, T. Inami, K. Ohwada, Y. Murata, H. Nojiri, Y. Murakami, H. Ohta, W. Zhang, K. Yoshimura, High-magnetic-field X-ray absorption spectroscopy of field-induced valence transition in $YbInCu_4$, J. Phys. Soc. Jpn. 76 (3) (2007) 034702.

[108] Y.H. Matsuda, T. Nakamura, J.L. Her, S. Michimura, T. Inami, K. Kindo, T. Ebihara, Suppression of f-electron itinerancy in $CeRu_2Si_2$ by a strong magnetic field, Phys. Rev. B 86 (July 2012) 041109.

[109] J.A. Mydosh, P.M. Oppeneer, *Colloquium*: Hidden order, superconductivity, and magnetism: The unsolved case of URu_2Si_2, Rev. Modern Phys. 83 (Nov 2011) 1301–1322.

[110] Hiroaki Kusunose, Hisatomo Harima, On the hidden order in URu_2Si_2, antiferro hexadecapole order and its consequences, J. Phys. Soc. Jpn. 80 (8) (2011) 084702.

[111] H. Amitsuka, K. Matsuda, I. Kawasaki, K. Tenya, M. Yokoyama, C. Sekine, N. Tateiwa, T.C. Kobayashi, S. Kawarazaki, H. Yoshizawa, Pressure–temperature phase diagram of the heavy-electron superconductor, in: Proceedings of the 17th International Conference on Magnetism, J. Magn. Magn. Mater. 310 (2, Part 1) (2007) 214–220.

[112] A. Suslov, J.B. Ketterson, D.G. Hinks, D.F. Agterberg, Bimal K. Sarma, H–T phase diagram of URu_2S_2 in high magnetic fields, Phys. Rev. B 68 (July 2003) 020406.

[113] Liam Malone, Tatsuma D. Matusda, Arlei Antunes, Georg Knebel, Valentin Taufour, Dai Aoki, Kamran Behnia, Cyril Proust, Jacques Flouquet, Thermoelectric evidence for high-field anomalies in the hidden order phase of URu_2Si_2, Phys. Rev. B 83 (June 2011) 245117.

[114] Kiyohiro Sugiyama, Miho Nakashima, Hitoshi Ohkuni, Koichi Kindo, Yoshinori Haga, Tetsuo Honma, Etsuji Yamamoto, Yoshichika Ōnuki, Metamagnetic transition in a heavy fermion superconductor URu_2Si_2, J. Phys. Soc. Jpn. 68 (10) (1999) 3394–3401.

[115] A.LeR. Dawson, W.R. Datars, J.D. Garrett, F.S. Razavi, Electrical transport in URu_2Si_2, J. Phys., Condens. Matter 1 (38) (1989) 6817.

[116] Y. Kasahara, T. Iwasawa, H. Shishido, T. Shibauchi, K. Behnia, Y. Haga, T.D. Matsuda, Y. Onuki, M. Sigrist, Y. Matsuda, Exotic superconducting properties in the electron-hole-compensated heavy-fermion "semimetal" URu_2Si_2, Phys. Rev. Lett. 99 (Sept 2007) 116402.

[117] Romain Bel, Hao Jin, Kamran Behnia, Jacques Flouquet, Pascal Lejay, Thermoelectricity of URu_2Si_2: Giant Nernst effect in the hidden-order state, Phys. Rev. B 70 (Dec 2004) 220501.

[118] Andres F. Santander-Syro, Markus Klein, Florin L. Boariu, Andreas Nuber, Pascal Lejay, Friedrich Reinert, Fermi-surface instability at the 'hidden-order' transition of URu_2Si_2, Nature Phys. 5 (9) (2009) 637–641.

[119] E. Hassinger, G. Knebel, T.D. Matsuda, D. Aoki, V. Taufour, J. Flouquet, Similarity of the Fermi surface in the hidden order state and in the antiferromagnetic state of URu_2Si_2, Phys. Rev. Lett. 105 (Nov 2010) 216409.

[120] Y.J. Jo, L. Balicas, C. Capan, K. Behnia, P. Lejay, J. Flouquet, J.A. Mydosh, P. Schlottmann, Pressure effect on the magnetic field–temperature (H–T) phase diagram of URu_2Si_2, Phys. B: Condens. Matter 403 (5–9) (2008) 749–751.

[121] H. Shishido, K. Hashimoto, T. Shibauchi, T. Sasaki, H. Oizumi, N. Kobayashi, T. Takamasu, K. Takehana, Y. Imanaka, T.D. Matsuda, Y. Haga, Y. Onuki, Y. Matsuda, Possible phase transition deep inside the hidden order phase of ultraclean URu_2Si_2, Phys. Rev. Lett. 102 (Apr 2009) 156403.

[122] M.M. Altarawneh, N. Harrison, S.E. Sebastian, L. Balicas, P.H. Tobash, J.D. Thompson, F. Ronning, E.D. Bauer, Sequential spin polarization of the Fermi surface pockets in URu_2S_2 and its implications for the hidden order, Phys. Rev. Lett. 106 (Apr 2011) 146403.

[123] Haruyoshi Aoki, Shinya Uji, Ariane Keiko Albessard, Yoshichika Ōnuki, Observation of heavy electrons in $CeRu_2Si_2$ via the dHvA effect, J. Phys. Soc. Jpn. 61 (10) (1992) 3457–3461.

[124] Yoshichika Ōnuki, Yoshinori Haga, Etsuji Yamamoto, Yoshihiko Inada, Rikio Settai, Hiroshi Yamagami, Hisatomo Harima, High-quality single crystal growth and the Fermi surface property of uranium and cerium compounds, J. Phys., Condens. Matter 15 (28) (2003) S1903.

[125] M. Springford, Heavy-fermion compounds, studied using the de Haas–van Alphen effect, Phys. B: Condens. Matter 171 (1–4) (1991) 151–160.

[126] Yu. Kagan, K.A. Kikoin, N.V. Prokof'ev, Effective-mass renormalization and de Haas–van Alphen effect in heavy-fermion systems, JETP Lett. 56 (4) (1992) 221–226.

[127] Yu. Kagan, K.A. Kikoin, N.V. Prokof'ev, Heavy fermions in the Kondo lattice as neutral quasiparticles and dHvA effect, Phys. B: Condens. Matter 194–196 (Part 1) (1994) 1171–1172.

[128] A.M. Tsvelik, New fermionic description of quantum spin liquid state, Phys. Rev. Lett. 69 (14) (Oct 1992) 2142–2144.

[129] N. Harrison, D.W. Hall, R.G. Goodrich, J.J. Vuillemin, Z. Fisk, Quantum interference in the spin-polarized heavy fermion compound CeB_6: Evidence for topological deformation of the Fermi surface in strong magnetic fields, Phys. Rev. Lett. 81 (4) (July 1998) 870–873.

[130] Jozef Spałek, Spin-split masses and a critical behavior of almost localized narrow-band and heavy-fermion systems, in: Proceedings of the International Conference on Strongly Correlated Electron Systems – SCES 2005, Phys. B: Condens. Matter 378–380 (2006) 654–660.

[131] Jozef Spałek, Magnetic properties of almost localized fermions revisited: Spin dependent masses and quantum critical behavior, Phys. Status Solidi (B) 243 (1) (2006) 78–88.

[132] Seiichiro Onari, Hiroshi Kontani, Yukio Tanaka, Spin-dependent mass enhancement under a magnetic field in the periodic Anderson model, J. Phys. Soc. Jpn. 77 (2) (2008) 023703.

[133] S. Viola Kusminskiy, K.S.D. Beach, A.H. Castro Neto, D.K. Campbell, Mean-field study of the heavy-fermion metamagnetic transition, Phys. Rev. B 77 (9) (Mar 2008) 094419.

[134] W. Joss, J.M. van Ruitenbeek, G.W. Crabtree, J.L. Tholence, A.P.J. van Deursen, Z. Fisk, Observation of the magnetic field dependence of the cyclotron mass in the Kondo lattice CeB_6, Phys. Rev. Lett. 59 (14) (Oct 1987) 1609–1612.

[135] C.D. Bredl, Specific heat of heavy fermions in Ce-based Kondo-lattices at very low temperatures, J. Magn. Magn. Mater. 63–64 (1987) 355–357.

[136] M. Endo, N. Kimura, A. Ochiai, H. Aoki, T. Terashima, C. Terakura, S. Uji, T. Matsumoto, Electronic structures of $PrPb_3$ in the para- and antiferroquadrupolar phases, Acta Phys. Polon. B 34 (22) (2003) 1031–1034.

[137] R.G. Goodrich, N. Harrison, A. Teklu, D. Young, Z. Fisk, Development of the high-field heavy-fermion ground state in $Ce_xLa_{1-x}B_6$ intermetallics, Phys. Rev. Lett. 82 (18) (May 1999) 3669–3672.

[138] R. Settai, H. Shishido, S. Ikeda, Y. Murakawa, M. Nakashima, D. Aoki, Y. Haga, H. Harima, Y. Onuki, Quasi-two-dimensional Fermi surfaces and the de Haas–van Alphen oscillation in both the normal and superconducting mixed states of $CeCoIn_5$, J. Phys., Condens. Matter 13 (27) (2001) L627–L634.

[139] Donavan Hall, E.C. Palm, T.P. Murphy, S.W. Tozer, Z. Fisk, U. Alver, R.G. Goodrich, J.L. Sarrao, P.G. Pagliuso, Takao Ebihara, Fermi surface of the heavy-fermion superconductor $CeCoIn_5$: The de Haas–van Alphen effect in the normal state, Phys. Rev. B 64 (21) (Nov 2001) 212508.

[140] A. McCollam, S.R. Julian, P.M.C. Rourke, D. Aoki, J. Flouquet, Anomalous de Haas–van Alphen oscillations in $CeCoIn_5$, Phys. Rev. Lett. 94 (18) (May 2005) 186401.

[141] Olga Howczaka, Jozef Spałek, Spin and magnetic field dependences of quasiparticle effective mass in ferromagnetic state of heavy fermions, in: SCES'11, Cambridge, UK, 2011.

[142] V.P. Mineev, K.V. Samokhin, De Haas–van Alphen effect in metals without an inversion center, Phys. Rev. B 72 (21) (Dec 2005) 212504.

[143] Arumugam Thamizhavel, Hiroaki Shishido, Yusuke Okuda, Hisatomo Harima, Tatsuma D. Matsuda, Yoshinori Haga, Rikio Settai, Yoshichika Ōnuki, Fermi surface property of $CeCoGe_3$ and $LaCoGe_3$ without inversion symmetry in the tetragonal crystal structure, J. Phys. Soc. Jpn. 75 (4) (2006) 044711.

[144] Ilya Sheikin, Pierre Rodiere, Rikio Settai, Yoshichika Ōnuki, High-field de Haas–van Alphen effect in non-centrosymmetric $CeCoGe_3$ and $LaCoGe_3$, J. Phys. Soc. Jpn. 80 (Supplement A) (2011) SA020.

[145] Ø. Fischer, in: K.H.J. Buschow, E.P. Wohlfarth (Eds.), Magnetic Superconductors in Ferromagnetic Materials, vol. 5, Elsevier Science Publishers B.V., Amsterdam, 1990.
[146] D. Fay, J. Appel, Coexistence of p-state superconductivity and itinerant ferromagnetism, Phys. Rev. B 22 (7) (Oct 1980) 3173–3182.
[147] E.A. Yelland, S.M. Hayden, S.J.C. Yates, C. Pfleiderer, M. Uhlarz, R. Vollmer, H. v. Löhneysen, N.R. Bernhoeft, R.P. Smith, S.S. Saxena, N. Kimura, Superconductivity induced by spark erosion in $ZrZn_2$, Phys. Rev. B 72 (Dec 2005) 214523.
[148] Valentin Taufour, Alain Villaume, Dai Aoki, Georg Knebel, Jacques Flouquet, Magnetic field evolution of critical end point in UGe_2, J. Phys. Conf. Ser. 273 (1) (2011) 012017.
[149] Andrew Huxley, Ilya Sheikin, Eric Ressouche, Nolwenn Kernavanois, Daniel Braithwaite, Roberto Calemczuk, Jacques Flouquet, UGe_2: A ferromagnetic spin-triplet superconductor, Phys. Rev. B 63 (14) (Mar 2001) 144519.
[150] F. Hardy, A. Huxley, J. Flouquet, B. Salce, G. Knebel, D. Braithwaite, D. Aoki, M. Uhlarz, C. Pfleiderer, (P, T) phase diagram of the ferromagnetic superconductor URhGe, in: Proceedings of the International Conference on Strongly Correlated Electron Systems, Phys. B: Condens. Matter 359–361 (2005) 1111–1113.
[151] Atsushi Miyake, Dai Aoki, Jacques Flouquet, Pressure evolution of the ferromagnetic and field re-entrant superconductivity in URhGe, J. Phys. Soc. Jpn. 78 (6) (2009) 063703.
[152] Elena Hassinger, Dai Aoki, Georg Knebel, Jacques Flouquet, Pressure–temperature phase diagram of polycrystalline UCoGe studied by resistivity measurement, J. Phys. Soc. Jpn. 77 (7) (2008) 073703.
[153] V. Taufour, D. Aoki, G. Knebel, J. Flouquet, Tricritical point and wing structure in the itinerant ferromagnet UGe_2, Phys. Rev. Lett. 105 (Nov 2010) 217201.
[154] Hisashi Kotegawa, Valentin Taufour, Dai Aoki, Georg Knebel, Jacques Flouquet, Evolution toward quantum critical end point in UGe_2, J. Phys. Soc. Jpn. 80 (8) (2011) 083703.
[155] Dai Aoki, Tristan Combier, Valentin Taufour, Tatsuma D. Matsuda, Georg Knebel, Hisashi Kotegawa, Jacques Flouquet, Ferromagnetic quantum critical endpoint in UCoAl, J. Phys. Soc. Jpn. 80 (9) (2011) 094711.
[156] T. Terashima, T. Matsumoto, C. Terakura, S. Uji, N. Kimura, M. Endo, T. Komatsubara, H. Aoki, Evolution of quasiparticle properties in UGe_2 with hydrostatic pressure studied via the de Haas–van Alphen effect, Phys. Rev. Lett. 87 (Sept 2001) 166401.
[157] R. Settai, M. Nakashima, S. Araki, Y. Haga, T.C. Kobayashi, N. Tateiwa, H. Yamagami, Y. Onuki, A change of the Fermi surface in UGe_2 across the critical pressure, J. Phys., Condens. Matter 14 (1) (2002) L29.
[158] N. Tateiwa, T.C. Kobayashi, K. Hanazono, K. Amaya, Y. Haga, R. Settai, Y. Onuki, Pressure-induced superconductivity in a ferromagnet UGe_2, J. Phys., Condens. Matter 13 (1) (2001) L17.
[159] M. Uhlarz, C. Pfleiderer, S.M. Hayden, Quantum phase transitions in the itinerant ferromagnet $ZrZn_2$, Phys. Rev. Lett. 93 (Dec 2004) 256404.
[160] R.A. Borzi, S.A. Grigera, J. Farrell, R.S. Perry, S.J.S. Lister, S.L. Lee, D.A. Tennant, Y. Maeno, A.P. Mackenzie, Formation of a nematic fluid at high fields in $Sr_3Ru_2O_7$, Science 315 (5809) (2007) 214–217.
[161] H. Kotegawa, A. Harada, S. Kawasaki, Y. Kawasaki, Y. Kitaoka, Y. Haga, E. Yamamoto, Y. Ōnuki, K.M. Itoh, E.E. Haller, H. Harima, Evidence for uniform coexistence of ferromagnetism and unconventional superconductivity in UGe_2: A ^{73}Ge-NQR study under pressure, J. Phys. Soc. Jpn. 74 (2) (2005) 705–711.
[162] Dai Aoki, Jacques Flouquet, Ferromagnetism and superconductivity in uranium compounds, J. Phys. Soc. Jpn. 81 (1) (2012) 011003.
[163] I. Sheikin, A. Huxley, D. Braithwaite, J.P. Brison, S. Watanabe, K. Miyake, J. Flouquet, Anisotropy and pressure dependence of the upper critical field of the ferromagnetic superconductor UGe_2, Phys. Rev. B 64 (Nov 2001) 220503.
[164] Dai Aoki, Frédéric Hardy, Atsushi Miyake, Valentin Taufour, Tatsuma D. Matsuda, Jacques Flouquet, Properties of ferromagnetic superconductors, C. R. Phys. 12 (5–6) (2011) 573–583.
[165] F. Hardy, D. Aoki, C. Meingast, P. Schweiss, P. Burger, H. v. Löhneysen, J. Flouquet, Transverse and longitudinal magnetic-field responses in the Ising ferromagnets URhGe, UCoGe, and UGe_2, Phys. Rev. B 83 (May 2011) 195107.
[166] Dai Aoki, Tatsuma D. Matsuda, Frédéric Hardy, Christoph Meingast, Valentin Taufour, Elena Hassinger, Ilya Sheikin, Carley Paulsen, Georg Knebel, Hisashi Kotegawa, Jacques Flouquet, Superconductivity reinforced by magnetic field and the magnetic instability in uranium ferromagnets, J. Phys. Soc. Jpn. 80 (Supplement A) (2011) SA008.
[167] Dai Aoki, Tatsuma D. Matsuda, Valentin Taufour, Elena Hassinger, Georg Knebel, Jacques Flouquet, Extremely large and anisotropic upper critical field and the ferromagnetic instability in UCoGe, J. Phys. Soc. Jpn. 78 (11) (2009) 113709.
[168] E. Slooten, T. Naka, A. Gasparini, Y.K. Huang, A. de Visser, Enhancement of superconductivity near the ferromagnetic quantum critical point in UCoGe, Phys. Rev. Lett. 103 (Aug 2009) 097003.
[169] S. Kittaka, http://sakaki.issp.u-tokyo.ac.jp/user/kittaka/contents/others/tc-history.html.
[170] N. Kimura, T. Sugawara, H. Aoki, T. Terashima, Novel superconducting properties on noncentrosymmetric heavy fermion $CeRhSi_3$, Phys. C Supercond. 470 (Supplement 1) (2010) S529–S532.
[171] Atsushi Miyake, Dai Aoki, Jacques Flouquet, Field re-entrant superconductivity induced by the enhancement of effective mass in URhGe, J. Phys. Soc. Jpn. 77 (9) (2008) 094709.
[172] Dai Aoki, Ilya Sheikin, Tatsuma D. Matsuda, Valentin Taufour, Georg Knebel, Jacques Flouquet, First observation of quantum oscillations in the ferromagnetic superconductor UCoGe, J. Phys. Soc. Jpn. 80 (1) (2011) 013705.
[173] Ed Yelland, Jack Barraclough, Weiwei Wang, Konstantin Kamenev, Andrew Huxley, High-field superconductivity at an electronic topological transition in URhGe, Nature Phys. 7 (2011) 890–894.
[174] Liam Malone, Ludovic Howald, Alexandre Pourret, Dai Aoki, Valentin Taufour, Georg Knebel, Jacques Flouquet, Thermoelectricity of the ferromagnetic superconductor UCoGe, Phys. Rev. B 85 (Jan 2012) 024526.
[175] T. Hattori, Y. Ihara, Y. Nakai, K. Ishida, Y. Tada, S. Fujimoto, N. Kawakami, E. Osaki, K. Deguchi, N.K. Sato, I. Satoh, Superconductivity induced by longitudinal ferromagnetic fluctuations in UCoGe, Phys. Rev. Lett. 108 (2012) 066403.
[176] H. Sakai, S. Kambe, Y. Tokunaga, Y. Haga, S.-H. Baek, F. Ronning, E.D. Bauer, J.D. Thompson, Anisotropy of antiferromagnetic spin fluctuations in the heavy fermion superconductors of CeMIn5 and PuMGa5 (M = Co, Rh), Mater. Res. Bull. 1264 (2010) 69.